TABLE 1. Anti HIV-1 activity of novel SDP derivatives in PBMC[a]

Compound	IC_{50} value in p24 assay (nM)					
	HIV-1_{Ba-L} (R5)	HIV-1_{JRFL} (R5)	HIV-1_{MOKW} (R5)	HIV-1_{MM} ($R5_{MDR}$)	HIV-1_{JSL} ($R5_{MDR}$)	HIV-1_{NL4-3} (X4)
AK602	0.5 ± 0.3	0.2 ± 0.1	0.3 ± 0.2	0.7 ± 0.3	0.4 ± 0.2	>1,000
TAK779	14 ± 5	6 ± 2	9 ± 3	12 ± 4	10 ± 3	>1,000
SCH-C	3 ± 2	2 ± 1	2 ± 1.5	2.5 ± 1	2 ± 1	>1,000
ZDV	13 ± 5	7 ± 3	10 ± 6	520 ± 75	64 ± 13	9 ± 5
SQV	8 ± 3	6 ± 2	6 ± 3	212 ± 56	276 ± 44	10 ± 4

[a] IC_{50}s were determined by using PHA-PBMC isolated from three different donors, and the inhibition of p24 Gag protein production was used as an endpoint. All assays were conducted in triplicate. The results shown represent arithmetic means (±1 standard deviation) of three independently conducted assays. HIV-1_{MOKW} was isolated from a drug-naive AIDS patient, and HIV-1_{JSL} and HIV-1_{MM} were isolated from patients who received antiretroviral therapy for a long period of time and whose virus loads showed a number of RT and PR mutations. Two previously published CCR5 inhibitors, TAK779 and SCH-C, and zidovudine (ZDV) and saquinavar (SQV) were used as reference compounds.

45.1%]), resulting in the ratios of 1.43 and 1.40 (Fig. 5C and D), respectively. Figure 6A illustrates the overall profiles of $CD4^+/CD8^+$ cells ratios on day 16 in the four groups. The mean $CD4^+/CD8^+$ cell ratio in mice (n = 7) given saline was 0.1 (range, 0.06 to 0.20). In contrast, the ratios in AK602-treated mice (n = 8) were significantly higher with a mean value of 0.92 (range, 0.23 to 1.89; P = 0.001), which was comparable to that in ddI-treated mice (n = 9; mean, 1.29; range, 0.38 to 2.68; P = 0.001) and uninfected mice (n = 7; mean, 1.0; range, 0.50 to 1.49). The numbers of $CD4^+$ cells/μl

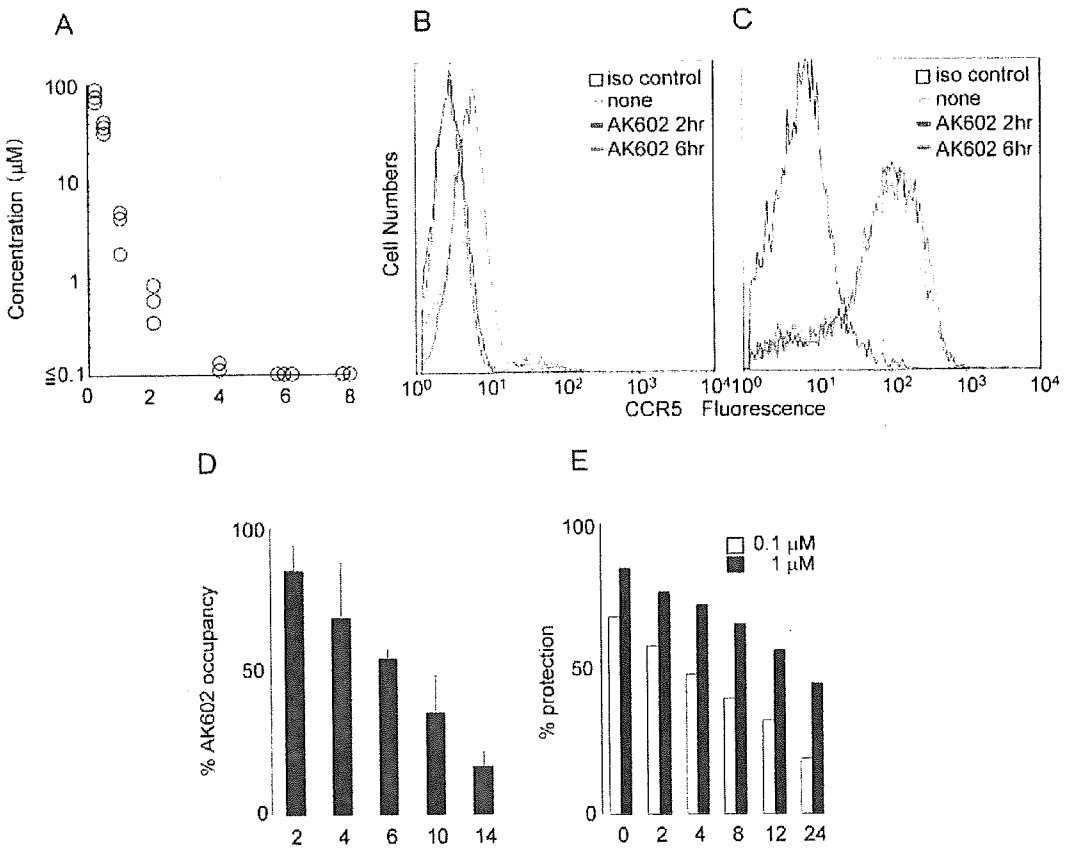

FIG. 4. Pharmacokinetics and persistence of anti-HIV-1 activity of AK602. (A) Pharmacokinetics of AK602. Each mouse was administered AK602 at a dose of 60 mg/kg, and blood samples were taken at 15, 30, 60, 120, 240, 480, and 720 min. Plasma concentrations of AK602 determined by HPLC analysis at 15, 30, 60, 120, and 240 min were 76.2, 36.1, 3.5, 0.6, and 0.13 μM, respectively. AK602 was not detected at later time points. (B and C) No CCR5 internalization or shedding was caused by AK602. Human PBMC were recovered 2 and 6 h after AK602 administration and stained with 45531 (B) or 3A9 (C). (D) Sustained AK602 occupancy on cell surfaces. At indicated periods of time after a bolus of AK-602 (60 mg/kg) was administered to hu-PBMC-NOG mice, PBMC were recovered and the percentages of AK602 occupancy on cellular CCR5 were determined with fluorescein isothiocyanate-conjugated monoclonal antibody 45531. (E) Persistence of in vitro activity of AK602 against R5 HIV-1 after AK602 depletion. $CCR5^+$ MAGI cells were exposed to 0.1 or 1 μM AK602 for 30 min and thoroughly washed to deplete AK602 from the medium. The cells were subsequently cultured for the indicated periods of time, exposed to HIV-1_{Ba-L}, and further cultured for 48 h, when the cells were harvested and lysed with Triton X-100-containing PBS. A solution containing chlorophenol red-β-D-galactopyranoside was added, the optical density was measured, and the percentage of protection was determined.

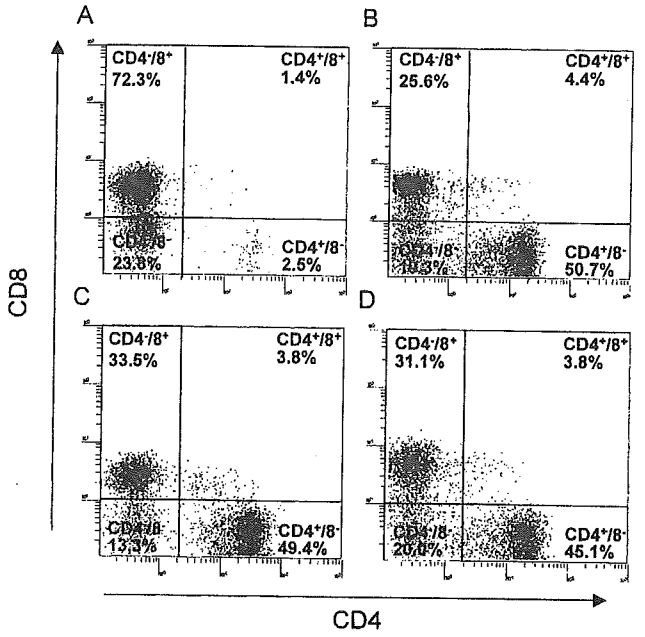

FIG. 5. Effects of AK602 on $CD4^+$ and $CD8^+$ cell counts in infected hu-PBMC-NOG mice. PBMC recovered on day 16 after R5 HIV-1 inoculation were subjected to flow cytometry. Shown are representative flow cytometric analysis profiles. Note that only 3.9% of $CD4^+$ cells were seen (A), resulting in a $CD4^+/CD8^+$ cell ratio of 0.05 in a mouse given saline, while distinct numbers of $CD4^+$ cells (55.1 and 53.2%) (B and C) were seen in AK602- and ddI-administered infected mice, resulting in $CD4^+/CD8^+$ cell ratios of 1.84 and 1.43, respectively. In an uninfected mouse (D), 48.9% of cells were positive for CD4, with a $CD4^+/CD8^+$ cell ratio of 1.40.

in saline-treated mice were significantly less than those of AK602-treated, ddI-treated, or uninfected mice (Fig. 6B).

Effects of AK602 on R5 HIV-1 proviral DNA copy numbers and serum p24 levels in R5 HIV-1-infected hu-PBMC-NOG mice. We next asked which population harbored proviral DNA in the cells recovered from R5 HIV-1-infected hu-PBMC-NOG mice, by purifying $CD4^+$ and $CD4^-$ cell populations and determining proviral DNA copy numbers in each population. As shown in Table 2, more than 99% of proviral DNA was found in $CD4^+$ cells and <0.3% of proviral DNA was detected in $CD4^-$ cells derived from saline-treated mice, indicating that R5 HIV-1 infection occurred in $CD4^+$ cells in the hu-PBMC-transplanted NOG environment. As illustrated in Fig. 6C, the mean number of R5 HIV-1 proviral DNA copies was 2.0×10^5 (range, 2.6×10^4 to 1.7×10^6) per 10^5 $CD4^+$ cells in R5 HIV-1-infected mice ($n = 7$) given saline. However, values for mice in groups given AK602 and ddI were 1.3×10^3 (range, 2.3×10^2 to 7.9×10^3; $P = 0.001$) and 1.8×10^2 (range, $<10^2$ to 7.9×10^2; $P = 0.001$), respectively.

The amounts of R5 HIV-1 p24 in serum were also found to be very high in saline-treated mice, with a mean amount of 1.1×10^5 pg/ml (range, 3.1×10^4 to 2.8×10^5 pg/ml). AK602 and ddI were found to significantly suppress the serum p24 amounts as examined on day 16 with a mean amount of 5.6×10^3 pg/ml (range, 8.1×10^2 to 2.1×10^4 pg/ml; $P = 0.001$) and 7.1×10^2 pg/ml (range, 1.3×10^2 to 1.1×10^4 pg/ml; $P = 0.001$), respectively (Fig. 6D).

AK602 suppressed R5 HIV-1 viremia in hu-PBMC-NOG mice. As described above, the PBMC transplanted to NOG mice were intensely activated in the xenogeneic environment and had undergone ~4 cycles of proliferation by day 2; a majority of the cells had undergone ≥10 cycles of proliferation by day 4 (Fig. 3B). These data suggested that R5 HIV-1 might extensively replicate in the hu-PBMC-NOG mice immediately after R5 HIV-1 inoculation. When we collected blood samples on days 5, 9, and 16 following the inoculation and determined R5 HIV-1 RNA copy numbers in infected, saline-treated mice ($n = 7$), the geometric mean copy number was 8.6×10^3/ml (range, 1.7×10^3 to 1.0×10^5) on day 5 and rapidly increased to 1.9×10^5/ml (range, 2.2×10^4 to 3.0×10^6) on day 9; by day 16, the mean copy number had reached 7.7×10^5/ml (range, 2.6×10^5 to 3.0×10^6/ml). However, AK602 significantly suppressed viremia by ~1.1 log, as examined on day 5; the mean numbers of R5 HIV-1 RNA copies in AK602-administered mice were 1.6 and 1.8 logs lower than those in saline-treated mice examined on days 9 and 16, respectively (Fig. 7). Comparable viremia suppression was seen in the mice receiving ddI (Fig. 7). It was noted that although AK602 did not completely prevent the viremia from further increasing after day 5, there was a clear reduction in the viremia increase rates. The mean slopes (change in RNA copies per day over the range of data from 5 to 16 days) for the group receiving saline was 0.167 ± 0.042, whereas those for the AK602 and ddI groups were 0.102 ± 0.041 and 0.091 ± 0.037, respectively. Thus, the rates of increase in the AK602 ($P = 0.0057$) and ddI ($P = 0.0023$) mice were significantly lower than that for the mice given saline, indicating that both of the agents significantly inhibited R5 HIV-1 replication in this mouse model over the range of days evaluated. No apparent AK602- or ddI-associated adverse effects were seen throughout the study period.

DISCUSSION

In the present hu-PBMC-NOG mouse model, human $CD4^+/CD8^+$ cell ratios went down to 0.1 by 16 days after R5 HIV-1 inoculation, the amounts of proviral DNA and p24 gag antigen reached 10^5 to 10^6 copies/10^5 $CD4^+$ cells and 10^5 pg/ml, respectively (Fig. 6), and no mice failed to be infected with R5 HIV-1. It is noteworthy that the use of NOG mice provides a higher engraftment rate than with other SCID mice such as NOD/Shi-SCID mice treated with anti-NK cell antibody or the β_2-microglobulin-deficient NOD-SCID mice (10). With NOG mice, the chimeric rate of 30 to 40% is achieved, and cord blood $CD34^+$ cells have been shown to "take" with as few as 100 cells (10). Moreover, all infected mice developed high levels of R5 HIV-1 viremia by day 16, reaching as high as 10^6 copies/ml (Fig. 7). It is worth noting that the notably high levels of HIV-1 viremia seen in the present mouse model by 16 days after R5 HIV-1 exposure can be seen only on acute infection or up to 10 years after HIV infection in humans (3, 4).

In the present study, we found that the conspicuous susceptibility to the infectivity and replication of R5 HIV-1 in these mice appeared to stem from the hyperactivation of the implanted human PBMC. The implanted PBMC were highly activated in the xenogeneic environment, expressed quite high

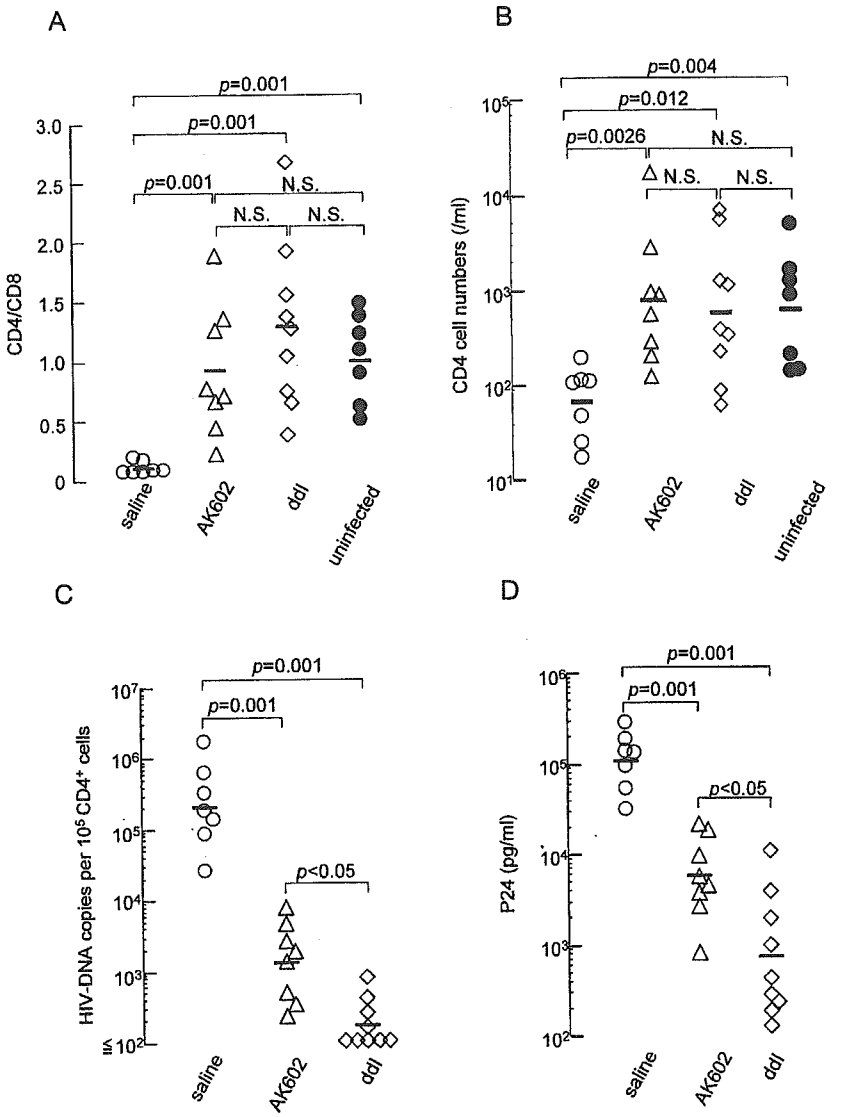

FIG. 6. Effects of AK602 on $CD4^+/CD8^+$ ratios and the amounts of proviral DNA and HIV-1 p24 in infected hu-PBMC-NOG mice. (A) Overall profiles of $CD4^+/CD8^+$ cell ratios. Note that the mean $CD4^+/CD8^+$ cell ratio in mice given saline ($n = 7$) was 0.1, while those in mice given AK602 or ddI were 0.92 and 1.29, respectively. The mean ratio in uninfected mice was 1.0. (B) Numbers of $CD4^+$ cells per microliter in each mouse group. (C) HIV-1 proviral DNA copy numbers in $CD4^+$ cells from each mouse group were determined by real-time PCR assay. Values are shown per 10^5 $CD4^+$ cells, as described in Materials and Methods. Note that the mean number of HIV-1 proviral DNA copies was 2.0×10^5 per 10^5 $CD4^+$ cells in mice given saline, while those in AK602- and ddI-treated groups were 1.3×10^3 and 1.8×10^2 per 10^5 $CD4^+$ cells (both, $P = 0.001$), respectively. (D) Amounts of plasma p24 antigen. Note that the amounts of p24 in plasma were high in saline-treated mice while AK602 and ddI significantly suppressed the serum p24 amounts as examined on day 16 after $HIV\text{-}1_{Ba\text{-}L}$ inoculation. The short bars indicate the arithmetic (A) and geometric (B, C, and D) means obtained.

levels of HLA-DR, and rapidly and continuously proliferated immediately after intraperitoneal infusion (Fig. 3A, B, and D). Moreover, the implanted PBMC expressed as much as 2.8-fold-higher levels of CCR5 on day 3 following implantation compared to PHA-PBMC on day 3 in culture (Fig. 3E). The combination of rapid proliferation and high levels of CCR5 expression of the implanted PBMC should explain the reason R5 HIV-1 rapidly replicated in the hu-PBMC-NOG mice and presented such high levels of R5 HIV-1 viremia. In this regard, only a few groups to date have documented the levels of viremia in the scientific literature. Among them are those by Garaci et al. (8) and Koyanagi et al. (14). The former documented high levels of viremia with a peak of 2.67×10^6 copies/ml in hu-PBL-NOD-SCID mice in which HIV-1-infected macrophages were inoculated, unlike our NOG mouse model where HIV-1 was directly inoculated. The latter report by Koyanagi et al. does not have viremia data but has data on p24 levels with a geometric mean of 11,092 pg/ml on day 14 after HIV-1 inoculation. However, the variation was much greater (178 to 1,434,444 pg/ml). Thus, one can say that the present model provides a greater reproducibility of high viremia levels than the mouse system reported by Koyanagi (14). It should be noted that the high levels of viremia and high engraftment rate achieved in this mouse model made it possible to monitor the

TABLE 2. Comparison of HIV-1 proviral DNA in human $CD4^+$ and $CD4^-$ cell fractions[a]

Sample	HIV-1 DNA copies (10^5 cells)		
	SCID-PBMC	$CD4^+$ cells	$CD4^-$ cells
Saline 1	138,858	162,193	461
Saline 2	135,967	117,949	<100
Saline 3	83,863	94,590	<100
AK602 1	3,390	2,300	<100
AK602 2	5,575	4,606	<100
AK602 3	1,925	1,398	<100
ddI 1	301	516	<100
ddI 2	793	1,317	<100
ddI 3	<100	118	<100

[a] HIV-1 proviral DNA copy numbers were determined by real-time PCR assay of unseparated human PBMC and purified $CD4^+$ and $CD4^-$ cells, following recovery from hu-PBMC-NOG mice. Values are shown per 10^5 cells, as described in Materials and Methods.

changes in the viremia levels periodically in the same set of mice without sacrificing them, while most of the previously described SCID mouse models required mice to be sacrificed at each time point of testing (25, 29, 30) or needed further in vitro coculture of the PBMC recovered from the mice with freshly prepared uninfected target cells for an additional period of days (9, 34).

We demonstrated in this study that a novel SDP derivative, AK602, exerted highly potent activity against laboratory and primary R5 HIV-1 strains as well as MDR R5 HIV-1 variant with IC_{50} values of subnanomolar concentrations (Table 1). It should be noted that AK602 represents a novel SDP derivative, which binds to human CCR5 but not to human CXCR4, CCR1, CCR2, CCR3, CCR4 or murine CCR5; blocks the binding of MIP-1α to CCR5 with an extremely high affinity (K_d values of ~3 nM); potently blocks HIV-1-gp120/CCR5 binding; and exerts potent activity against a wide spectrum of laboratory and primary R5 HIV-1 isolates including MDR HIV-1 and HIV-1 strains of various clades with IC_{50} values of 0.2 to 0.6 nM in vitro (K. Maeda, H. Ogata, S. Harada, Y. Tojo, T. Miyakawa, H. Nakata, Y. Takaoka, S. Shibayama, D. Fukushima, J. Moravek, E. Arnold, and H. Mitsuya, 11th Conf. Retrovir. Opp. Infect., abstr. 540, 2004; J. Demarest et al., XV Int. AIDS Conf., abstr. WeOrA1231, 2004). The plasma half-life of AK602 in the hu-PBMC-NOG mice, however, proved to be as short as 29 min when the agent was administered intraperitoneally (Fig. 4A). Considering that AK602 possesses such a high binding affinity to CCR5, we presumed that AK602 could remain on CCR5 for an extended period of time even after the agent was removed from the bloodstream in mice. The high and extensive level of AK602 occupancy observed in PBMC recovered from mice receiving AK602 substantiated this presumption (Fig. 4D). The subsequent in vitro experiment in which $CCR5^+$ MAGI cells were incubated with AK602 but exposed to R5 HIV-1 after the removal of the compound from the culture medium showed that AK602's anti-R5 HIV-1 activity can persist for an extensive period of time even if AK602 is no longer present in the culture (Fig. 4E). It is of note that unlike certain reports of in vivo anti-HIV-1 activity of chemokine antagonists which were administered before HIV-1 inoculation, thus demonstrating prophylactic effects of such agents (9, 30), the present system demonstrates anti-HIV-1 treatment after the establishment of HIV-1 infection, analogous to antiviral therapy in clinical settings.

When highly active antiretroviral therapy exerts its potent antiviral effects in clinical settings, a decrease in HIV-1 viremia is seen often within weeks, ultimately resulting in undetectable viremia; however in the present study, the viremia levels in mice receiving AK602 or ddI continued to increase although the rate of increment significantly declined (Fig. 7). The failure of AK602 and ddI to decrease viremia levels could be due in part to such a rapid viral replication in hyperactivated and proliferating $CD4^+$ cells. As discussed earlier, PBMC recovered from the hu-PBMC-NOG mice were highly positive for CCR5 and HLA-DR (Fig. 3D and E), compared to the levels of activation seen in the same donor's PHA-PBMC. It should be noted, however, that the mean numbers of proviral DNA copies on day 16 in mice receiving AK602 and ddI were 1.3×10^3 and 1.8×10^2 per 10^5 $CD4^+$ cells, respectively (Fig. 6C), suggesting that most $CD4^+$ cells (98.7 and 99.8% on average, respectively) were free of HIV-1 and proliferating in those

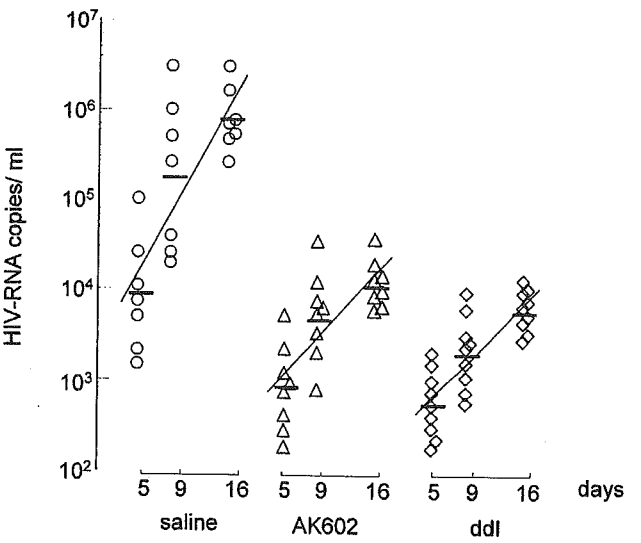

FIG. 7. AK602 suppresses R5 HIV-1 viremia in hu-PBMC-NOG mice. Blood samples were collected on days 5, 9, and 16 after inoculation and were subjected to the determination of R5 HIV-1 RNA copy numbers. Note that the copy numbers in saline-treated mice rapidly increased and reached ~10^6/ml by day 16, while AK602 significantly suppressed the viremia by 1.6 and 1.8 logs as examined on day 9 ($P = 0.001$ compared to saline-treated mice) and day 16 ($P = 0.001$), respectively. Comparable viremia suppression was seen in ddI-treated mice, except on day 16, when ddI activity was greater than that of AK602 ($P = 0.027$). Note that there was a clear reduction in the rate of increase of viremia as well. When the values of $\log_{10}$ HIV-1 RNA copies were calculated and the slopes corresponding to the rates of increase per day were determined, the resulting mean slope (solid line) for the saline-treated mice was 0.167 ± 0.042, whereas those for the AK602- and ddI-treated mice were 0.102 ± 0.041 and 0.091 ± 0.037, respectively. The increase rate for saline-treated mice was significantly higher than those of AK602-treated mice ($P = 0.0057$) and ddI-treated mice ($P = 0.0023$), respectively. The horizontal bars and solid lines represent the geometric means of HIV-1 RNA copy numbers and the slopes calculated, respectively.

mice on day 16 after the virus inoculation, if one copy of proviral DNA was postulated to reside in one $CD4^+$ cell.

One of us (Y.K.) previously attempted to investigate the mechanism of $CD4^+$ cell depletion seen in individuals with HIV-1 infection by employing a PBMC-transplanted NOD (NOD/Shi) *scid/scid* mouse system (24). Massive apoptosis was observed in HIV-1-uninfected $CD4^+$ cells in the spleens of the HIV-1-infected NOD-*scid/scid* mice. A combination of terminal deoxynucleotidyl transferase-mediated dUTP nick-end labeling and immunostaining for death-inducing tumor necrosis factor (TNF) family molecules showed that apoptotic cells were frequently found in conjugation with TNF-related apoptosis-inducing ligand (TRAIL)-expressing $CD3^+$ $CD4^+$ human T cells. Further observation that a neutralizing anti-TRAIL antibody inhibited the development of $CD4^+$ cell apoptosis suggested that a large number of HIV-1-uninfected $CD4^+$ cells undergo TRAIL-mediated apoptosis, contributing to the marked depletion of $CD4^+$ cells (24). The observation by Miura and his colleagues that the number of TRAIL-positive cells was consistently higher in HIV-1-infected mice than in uninfected ones makes it apparent that TRAIL expression is induced upon HIV-1 infection (23, 24). In this regard, the present observation that AK602 and ddI potently blocked the decrease in $CD4^+$ cells in spite of the rather increasing HIV-1 viremia in the face of AK602 or ddI (Fig. 7) suggests that the mere presence of viremia might not be sufficient for the HIV-induced apoptosis in $CD4^+$ cells. Our observation that most surviving $CD4^+$ cells in mice receiving AK602 or ddI were free of HIV-1 (see above) suggests that these anti-HIV-1 agents might block not only de novo HIV-1 infection, but also bystander killing of uninfected $CD4^+$ cells. The present data also suggest that a certain factor(s) such as cytokines produced by the freshly HIV-1-infected cells might mediate the apoptosis of bystander $CD4^+$ cells through the upregulation of TRAIL expression, death receptors (e.g., DR4 and DR5), and/or downregulation of decoy receptors (e.g., DcR1 and DcR2) (26, 27). However, experiments with a combination of terminal deoxynucleotidyl transferase-mediated dUTP nick-end labeling and TNF family molecules have to be conducted for better understanding of the bystander killing in regard to AK602's effects.

It is of note that several CCR5 antagonists are currently in various stages of development. AK602 has recently been administered to healthy adult subjects in a phase I clinical trial and shown to bind to CCR5 for an extended period of time, suggesting that an oral formulation with fewer administrations and lower dosage is possible for AK602 as a therapeutic agent for HIV-1 infection (J. Demarest, K. Adkison, S. Sparks, A. Shachoy-Clark, K. Schell, S. Reddy, L. Fang, K. O'Mara, S. Shibayama, and S. Piscitelli, 11th Conf. Retrovir. Opp. Infect., abstr. 139, 2004). Taken together, our observations that plasma viral load reached ~10^6 RNA copies/ml and that AK602 potently inhibited the replication of R5 HIV-1 strongly suggest that the present hu-PBMC-NOG mouse AIDS model could serve as a useful instrument for analyzing the pathogenesis of HIV-1 infection and testing the efficacy of antiviral agents.

ACKNOWLEDGMENTS

We thank Seth Steinberg for statistical analysis and Naoko Misawa, Yuji Kawano, and Hiromi Ogata for technical assistance and discussion.

This work was supported in part by grant-in-aids for Scientific Research on Priority Areas (14207025 and 15019086) from the Japanese Ministry of Education, Science, Sports, Culture and Technology of Japan (Monbu-Kagakusho) and a grant for AIDS Research (H15-AIDS-001) from the Ministry of Health, Labor, and Welfare of Japan (Kosei-Rohdosho).

REFERENCES

1. **Baba, M., O. Nishimura, N. Kanzaki, M. Okamoto, H. Sawada, Y. Iizawa, M. Shiraishi, Y. Aramaki, K. Okonogi, Y. Ogawa, K. Meguro, and M. Fujino.** 1999. A small-molecule, nonpeptide CCR5 antagonist with highly potent and selective anti HIV-1 activity. Proc. Natl. Acad. Sci. USA **96**:5698–5703.
2. **Carr, A., K. Samaras, A. Thorisdottir, G. R. Kaufmann, D. J. Chisholm, and D. A. Cooper.** 1999. Diagnosis, prediction, and natural course of HIV-1 protease-inhibitor associated lipodystrophy, hyperlipidaemia, and diabetes mellitus: a cohort study. Lancet **353**:2093–2099.
3. **Dean, M., M. Carrington, C. Winkler, G. A. Huttley, M. W. Smith, R. Allikmets, J. J. Goedert, S. P. Buchbinder, E. Vittinghoff, E. Gomperts, S. Donfield, D. Vlahov, R. Kaslow, A. Saah, C. Rinaldo, R. Detels, and S. J. O'Brien.** 1996. Genetic restriction of HIV-1 infection and progression to AIDS by a deletion allele of the CKR5 structural gene. Hemophilia Growth and Development Study, Multicenter AIDS Cohort Study, Multicenter Hemophilia Cohort Study, San Francisco City Cohort, ALIVE Study. Science **273**:1856–1862.
4. **Easterbrook, P. J.** 1999. Long-term non-progression in HIV infection: definitions and epidemiological issues. J. Infect. **38**:71–73.
5. **Fauci, A. S.** 1999. The AIDS epidemic—considerations for the 21st century. N. Engl. J. Med. **341**:1046–1050.
6. **Finzi, D., J. Blankson, J. D. Siliciano, J. B. Margolick, K. Chadwick, T. Pierson, K. Smith, J. Lisziewicz, F. Lori, C. Flexner, T. C. Quinn, R. E. Chaisson, E. Rosenberg, B. Walker, S. Gange, J. Gallant, and R. F. Siliciano.** 1999. Latent infection of CD4+ T cells provides a mechanism for lifelong persistence of HIV-1, even in patients on effective combination therapy. Nat. Med. **5**:512–517.
7. **Gartner, S., P. Markovits, D. M. Markovitz, M. H. Kaplan, R. C. Gallo, and M. Popovic.** 1986. The role of mononuclear phagocytes in HTLV-III/LAV infection. Science **233**:215–219.
8. **Garaci, E., S. Aquaro, C. Lapenta, A. Amendola, M. Spada, S. Covaceuszach, C. F. Perno, and F. Belardelli.** 2003. Anti-nerve growth factor Ab abrogates macrophage-mediated HIV-1 infection and depletion of CD4+ T lymphocytes in hu-SCID mice. Proc. Natl. Acad. Sci. USA **100**:8927–8932.
9. **Ichiyama, K., S. Yokoyama-Kumakura, Y. Tanaka, R. Tanaka, K. Hirose, K. Bannai, T. Edamatsu, M. Yanaka, Y. Niitani, N. Miyano-Kurosaki, H. Takaku, Y. Koyanagi, and N. Yamamoto.** 2003. A duodenally absorbable CXC chemokine receptor 4 antagonist, KRH-1636, exhibits a potent and selective anti-HIV-1 activity. Proc. Natl. Acad. Sci. USA **100**:4185–4190.
10. **Ito, M., H. Hiramatsu, K. Kobayashi, K. Suzue, M. Kawahata, K. Hioki, Y. Ueyama, Y. Koyanagi, K. Sugamura, K. Tsuji, T. Heike, and T. Nakahata.** 2002. NOD/SCID/γ(c)(null) mouse: an excellent recipient mouse model for engraftment of human cells. Blood **100**:3175–3182.
11. **Kavlick, M. F., and H. Mitsuya.** 2001. The emergence of drug resistant HIV-1 variants and its impact on antiretroviral therapy of HIV-1 infection, p. 279–312. *In* E. De Clercq (ed.), The art of antiretroviral therapy. American Society for Microbiology, Washington, D.C.
12. **Koh, Y., H. Nakata, K. Maeda, H. Ogata, G. Bilcer, T. Devasamudram, J. F. Kincaid, P. Boross, Y. F. Wang, Y. Tie, P. Volarath, L. Gaddis, R. W. Harrison, I. T. Weber, A. K. Ghosh, and H. Mitsuya.** 2003. Novel bis-tetrahydrofuranylurethane-containing nonpeptidic protease inhibitor (PI) UIC-94017 (TMC114) with potent activity against multi-PI-resistant human immunodeficiency virus in vitro. Antimicrob. Agents Chemother. **47**:3123–3129.
13. **Koyanagi, Y., S. Miles, R. T. Mitsuyasu, J. E. Merrill, H. V. Vinters, and I. S. Chen.** 1987. Dual infection of the central nervous system by AIDS viruses with distinct cellular tropisms. Science **236**:819–822.
14. **Koyanagi, Y., Y. Tanaka, J. Kira, M. Ito, K. Hioki, N. Misawa, Y. Kawano, K. Yamasaki, R. Tanaka, Y. Suzuki, Y. Ueyama, E. Terada, T. Tanaka, M. Miyasaka, T. Kobayashi, Y. Kumazawa, and N. Yamamoto.** 1997. Primary human immunodeficiency virus type 1 viremia and central nervous system invasion in a novel hu-PBL-immunodeficient mouse strain. J. Virol. **71**:2417–2424.
15. **Lee, B., M. Sharron, L. J. Montaner, D. Weissman, and R. W. Doms.** 1999. Quantification of CD4, CCR5, and CXCR4 levels on lymphocyte subsets, dendritic cells, and differentially conditioned monocyte-derived macrophages. Proc. Natl. Acad. Sci. USA **96**:5215–5220.
16. **Lyons, A. B.** 2000. Analysing cell division in vivo and in vitro using flow cytometric measurement of CFSE dye dilution. J. Immunol. Methods **243**: 147–154.
17. **Maeda, K., K. Yoshimura, S. Shibayama, H. Habashita, H. Tada, K. Sagawa, T. Miyakawa, M. Aoki, D. Fukushima, and H. Mitsuya.** 2001. Novel low molecular weight spirodiketopiperazine derivatives potently inhibit R5

HIV-1 infection through their antagonistic effects on CCR5. J. Biol. Chem. 276:35194–35200.
18. **Maeda, Y., M. Foda, S. Matsushita, and S. Harada.** 2000. Involvement of both the V2 and V3 regions of the CCR5-tropic human immunodeficiency virus type 1 envelope in reduced sensitivity to macrophage inflammatory protein 1α. J. Virol. 74:1787–1793.
19. **McCune, J. M., R. Namikawa, C. C. Shih, L. Rabin, and H. Kaneshima.** 1990. Suppression of HIV infection in AZT-treated SCID-hu mice. Science 247:564–566.
20. **Mitsuya, H., and S. Broder.** 1986. Inhibition of the in vitro infectivity and cytopathic effect of human T-lymphotropic virus type III/lymphadenopathy virus-associated virus (HTLV-III/LAV) by 2′,3′-dideoxynucleosides. Proc. Natl. Acad. Sci. USA 83:1911–1915.
21. **Mitsuya, H., and S. Broder.** 1987. Strategies for antiviral therapy in AIDS. Nature 325:773–778.
22. **Mitsuya, H., and J. Erickson.** 1999. Discovery and development of antiretroviral therapeutics for HIV infection, p. 751–780. *In* T. C. Merigan, J. G. Bartlet, and D. Bolognesi (ed.), Textbook of AIDS medicine. Williams & Wilkins, Baltimore, Md.
23. **Miura, Y., N. Misawa, Y. Kawano, H. Okada, Y. Inagaki, N. Yamamoto, M. Ito, H. Yagita, K. Okumura, H. Mizusawa, and Y. Koyanagi.** 2003. Tumor necrosis factor-related apoptosis-inducing ligand induces neuronal death in a murine model of HIV central nervous system infection. Proc. Natl. Acad. Sci. USA 100:2777–2782.
24. **Miura, Y., N. Misawa, N. Maeda, Y. Inagaki, Y. Tanaka, M. Ito, N. Kayagaki, N. Yamamoto, H. Yagita, H. Mizusawa, and Y. Koyanagi.** 2001. Critical contribution of tumor necrosis factor-related apoptosis-inducing ligand (TRAIL) to apoptosis of human CD4+ T cells in HIV-1-infected hu-PBL-NOD-SCID mice. J. Exp. Med. 193:651–660.
25. **Mosier, D. E., R. J. Gulizia, S. M. Baird, D. B. Wilson, D. H. Spector, and S. A. Spector.** 1991. Human immunodeficiency virus infection of human-PBL-SCID mice. Science 251:791–794.
26. **Pan, G., J. Ni, Y. F. Wei, G. Yu, R. Gentz, and V. M. Dixit.** 1997. An antagonist decoy receptor and a death domain-containing receptor for TRAIL. Science 277:815–818.
27. **Pan, G., K. O'Rourke, A. M. Chinnaiyan, R. Gentz, R. Ebner, J. Ni, and V. M. Dixit.** 1997. The receptor for the cytotoxic ligand TRAIL. Science 276:111–113.
28. **Ratain, M., and W. Plunkett.** 1997. Pharmacology, p. 875–889. *In* J. Holland, R. Bast, Jr., D. Morton, E. Frei, D. KuFe, and R. Weichselbaum (ed.), Cancer medicine, 4th ed. Williams and Wilkins, Baltimore, Md.
29. **Ruxrungtham, K., E. Boone, H. Ford, Jr., J. S. Driscoll, R. T. Davey, Jr., and H. C. Lane.** 1996. Potent activity of 2′-β-fluoro-2′,3′-dideoxyadenosine against human immunodeficiency virus type 1 infection in hu-PBL-SCID mice. Antimicrob. Agents Chemother. 40:2369–2374.
30. **Strizki, J. M., S. Xu, N. E. Wagner, L. Wojcik, J. Liu, Y. Hou, M. Endres, A. Palani, S. Shapiro, J. W. Clader, W. J. Greenlee, J. R. Tagat, S. McCombie, K. Cox, A. B. Fawzi, C. C. Chou, C. Pugliese-Sivo, L. Davies, M. E. Moreno, D. D. Ho, A. Trkola, C. A. Stoddart, J. P. Moore, G. R. Reyes, and B. M. Baroudy.** 2001. SCH-C (SCH 351125), an orally bioavailable, small molecule antagonist of the chemokine receptor CCR5, is a potent inhibitor of HIV-1 infection in vitro and in vivo. Proc. Natl. Acad. Sci. USA 98:12718–12723.
31. **Walker, U. A., B. Setzer, and N. Venhoff.** 2002. Increased long-term mitochondrial toxicity in combinations of nucleoside analogue reverse-transcriptase inhibitors. AIDS 16:2165–2173.
32. **Westervelt, P., H. E. Gendelman, and L. Ratner.** 1991. Identification of a determinant within the human immunodeficiency virus 1 surface envelope glycoprotein critical for productive infection of primary monocytes. Proc. Natl. Acad. Sci. USA 88:3097–3101.
33. **Yahata, T., K. Ando, Y. Nakamura, Y. Ueyama, K. Shimamura, N. Tamaoki, S. Kato, and T. Hotta.** 2002. Functional human T lymphocyte development from cord blood CD34+ cells in nonobese diabetic/Shi-scid, IL-2 receptor gamma null mice. J. Immunol. 169:204–209.
34. **Yoshida, A., R. Tanaka, T. Murakami, Y. Takahashi, Y. Koyanagi, M. Nakamura, M. Ito, N. Yamamoto, and Y. Tanaka.** 2003. Induction of protective immune responses against R5 human immunodeficiency virus type 1 (HIV-1) infection in hu-PBL-SCID mice by intrasplenic immunization with HIV-1-pulsed dendritic cells: possible involvement of a novel factor of human CD4(+) T-cell origin. J. Virol. 77:8719–8728.
35. **Yoshimura, K., R. Kato, K. Yusa, M. F. Kavlick, V. Maroun, A. Nguyen, T. Mimoto, T. Ueno, M. Shintani, J. Falloon, H. Masur, H. Hayashi, J. Erickson, and H. Mitsuya.** 1999. JE-2147: a dipeptide protease inhibitor (PI) that potently inhibits multi-PI-resistant HIV-1. Proc. Natl. Acad. Sci. USA 96: 8675–8680.

Rev. Med. Virol. 2005; **15**: 169–178.
Published online 11 March 2005 in Wiley InterScience (www.interscience.wiley.com).
DOI: 10.1002/rmv.462
Reviews in Medical Virology

REVIEW

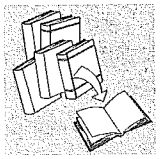

Death ligand-mediated apoptosis in HIV infection

Yoshiharu Miura* and Yoshio Koyanagi

Laboratory of Viral Pathogenesis, Research Center for AIDS, Institute for Virus Research, Kyoto University, Japan

SUMMARY

Apoptosis has been suggested to cause severe $CD4^+$ T cell depletion in patients infected with HIV. This review focuses on the biological events involved in death ligand-induced apoptosis during HIV infection. Among these ligands, TRAIL appears critical in HIV-infection. Death ligand-induced apoptosis might be a major pathogenic event in many virus-induced diseases including AIDS and the clarification of its mechanism will aid in the development of therapeutic strategies. Copyright © 2005 John Wiley & Sons, Ltd.

Received: 12 November 2004; Accepted: 15 November 2004

INTRODUCTION

Severe CD4 depletion is a hallmark of acquired immunodeficiency syndrome (AIDS) and the gradual loss of $CD4^+$ T cells leading to the onset of AIDS appears to be a result of infection with human immunodeficiency virus (HIV). Apoptosis, which has been shown to be significantly induced in HIV-infected individuals, seems to trigger the CD4 depletion during disease progression. Two major pathways have been identified from extensive molecular biology-based analysis; an extrinsic pathway, which is initiated by the binding of tumor-necrosis factor (TNF) family ligands to their cognate death receptors, and an intrinsic pathway, which is initiated by an internal sensor system that mainly transmits signals to the mitochondria and is mediated by Bcl-2-related proteins [1,2]. This review summarises our present level of understanding of the molecular mechanisms behind the extrinsic pathway of T lymphocyte apoptosis with HIV infection.

Corresponding author: Dr Y. Miura, Institute for Virus Research, Kyoto University, 53 Shougoin-kawaramachi, Sakyou-ku, Kyoto 606-8507, Japan. E-mail: ymiura@virus.kyoto-u.ac.jp

Abbreviations used

AICD, activation-induced cell death; AIDS, acquired immunodeficiency syndrome; cFLIP, cellular FLICE inhibitory protein; DISC, death-inducing signaling complex; FADD, Fas-associated death domain; FLICE, FADD-like ICE; HIV, human immunodeficiency virus; TNF, tumor necrosis factor; TRAIL, TNF-related apoptosis-inducing ligand.

HIV INFECTION AND APOPTOSIS

Apoptosis is thought to occur in HIV-infected individuals and arise from the following mechanisms; HIV-induced syncytium formation, HIV protein-induced cell death, activation-induced cell death (AICD) and bystander cell killing (Figure 1). Ballooning cells and multinucleic giant cells are frequently found in virus-infected cell cultures *in vitro*. The cytopathic effect (CPE) in HIV-infected $CD4^+$ T cell cultures is known to be the formation of syncytia between productively infected and adjacent uninfected cells and clearly induces the apoptosis in these cells, obviously dependent on viral replication [3,4]. Syncytia are also found in infected tissues [5,6]. The envelope glycoprotein complex of gp120-gp41 on the surface of the infected cells, which causes the death of both infected and adjacent uninfected cells, seems to be one of the dominant apoptosis-inducing molecules encoded by the HIV-1 genome (Figure 2). The envelope expressed on the plasma membrane of infected cells can interact with the CD4 molecule and a suitable co-receptor to trigger cell-to-cell fusion; resulting in syncytia and subsequently apoptosis [7,8]. It was reported that mitochondria-dependent apoptosis (intrinsic pathway) occurs with the fusion of envelope-expressing cells with CD4- and coreceptor-expressing target cells [9]. The shedding of HIV-encoded proteins such as envelope, Tat and Vpr (Figure 2) has also been shown to trigger apoptosis in both infected and

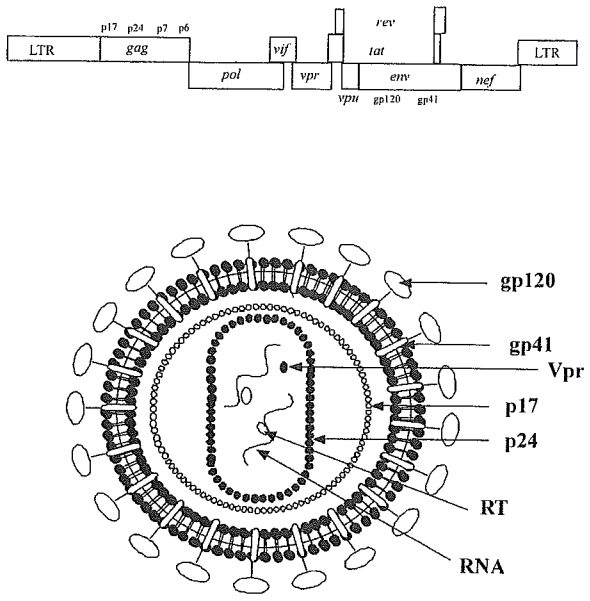

Figure 1. The HIV-1 provirus and its proteins. Gag and Gag-Pol polyprotein precursors are processed by the viral protease into nine subunits: protease, reverse transcriptase, integrase, matrix, capsid, p2, nucleocapsid, p1 and p6. Env is cleaved by cellular proteases, such as furin, into surface gp120 and transmembrane gp41 moieties. Tat is a transcriptional and translational regulator of expression. The RNA target region, the transactivation response (TAR) element, is located at the 5′ end of all viral transcripts. Rev has a major role in the nuclear-export of large HIV-1 RNA (gag and env transcripts) and regulates the shift between early and late viral gene expression. The viral-infectivity factor (Vif), viral protein u (Vpu), viral protein R (Vpr) and negative effector (Nef) proteins are known as accessory proteins because they are dispensable for viral growth in some cell-culture systems

uninfected cells in culture. Tat effectively induces apoptosis by downregulating the expression of Bcl-2 and upregulating the expression of Bax as well as caspase 8 [10,11]. On the other hand, the typical intrinsic pathway can be triggered by the soluble form of Vpr protein, which causes a rapid disintegration of the mitochondrial transmembrane potential in intact cells, as well as the release of cytochrome c and subsequent apoptosis [12]. On the other hand, AICD, which is known to be dependent on death receptors, was observed in *ex vivo* cultured T cells from HIV-infected patients following activation with mitogens, superantigens or antibodies specific for TCR [13]. AICD was originally found to occur during the elimination of prolongly activated T cells when the inflammatory reaction is coming to an end. Significantly, increased destruction of $CD4^+$ T cells in secondary lymphoid organs such as lymph nodes and spleen has been reported in HIV-infected individuals [14]. In addition, it has been postulated that HIV-1 infection causes uninfected $CD4^+$ T cells to die, and a bystander cell killing mechanism has been suggested based on histopathological analyses of lymph nodes in HIV-1-infected individuals and simian immunodeficiency virus (SIV)-infected monkeys [15]. The persistent existence of HIV proteins (Tat, gp120, Nef, Vpu) *in vivo* might stimulate apoptosis in uninfected bystander cells.

APOPTOSIS AND DEATH LIGAND

The extrinsic pathway arises from the binding of the ligand molecule to its respective membrane-bound death receptor and the engagement of the caspase cascade (Figure 3). Death receptors are members of the TNF receptor superfamily, which initiate a rapid activation of the caspase cascade and commit the cell to apoptosis when triggered by their cognate TNF family ligands. These ligands include Fas ligand (FasL), TNF, TNF-related apoptosis-inducing ligand (TRAIL) and TWEAK, and all of the death receptors possess both a cysteine-rich extracellular domain and an intracellular cytoplasmic sequence motif, known as the death domain (DD).

FasL is a type 2 membrane protein and an exclusive ligand for Fas, inducing Fas-mediated apoptosis [16]. The ligation of FasL to Fas triggers the Fas monomers to combine into trimeric Fas-complexes (Figure 3). The intracellular domain of Fas contains the DD, a stretch of 80 amino acids. After the trimerisation of Fas molecules, the DD recruits many cytosol proteins and forms a multi-protein death-inducing signaling complex (DISC) [17,18]. Immediately following Fas/FasL ligation, the prompt recruitment of a serine-phosphorylated adaptor molecule, Fas-associated DD (FADD), is induced and then the Fas/FADD interaction is coordinated through the highly conserved DD motifs found in both proteins. FADD serves as a bridge between Fas and downstream molecules, such as Fas-like IL-1β converting enzyme (FLICE) as well as cytotoxicity-dependent APO-1-associated protein 3 (CAP3). The FADD-FLICE/CAP3 interaction allows the liberation of caspase 8 and CAP3 in an active form from their dormant states. Formation of the DISC, which is composed of Fas, FADD and FLICE/CAP3, results in the initiation of a signal cascade to downstream target molecules, such as procaspase 3, 6 and 7. The activated

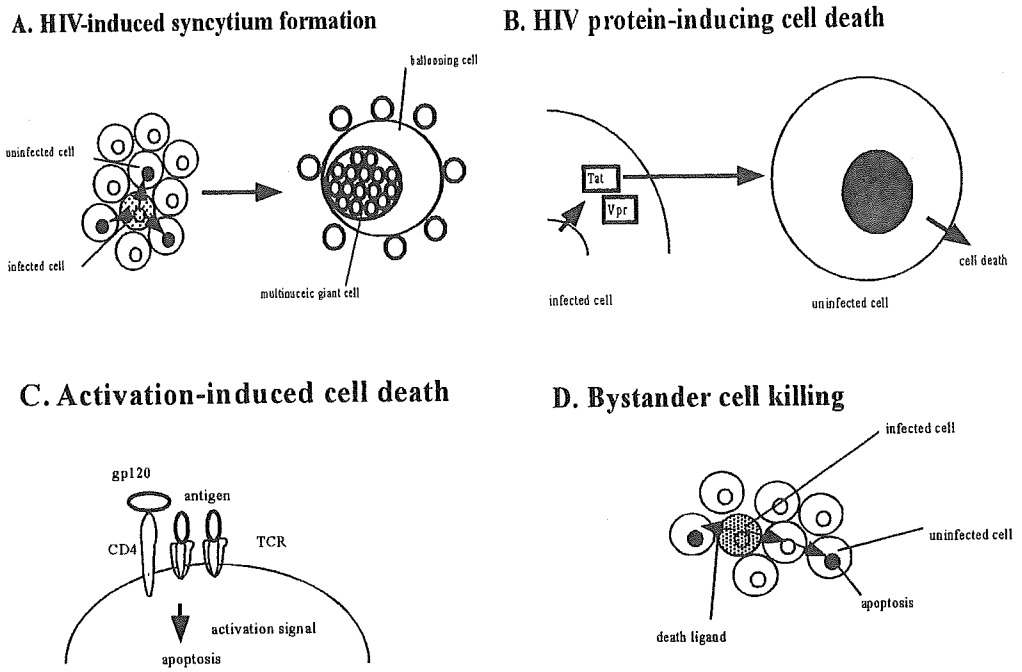

Figure 2. Mechanism of HIV-1-induced cell death. (A) HIV-induced syncytium formation arising from cell to cell fusion. (B) HIV protein-induced cell death. (C) Activation induced cell death through stimulation of TCR or gp120. (D) Bystander cell killing mediated by the death signal

form of caspase 3 efficiently cleaves a variety of cellular constituents, including the DNA repair enzymes, poly-ADP ribose polymerase and DNA-induced protein kinase, cytoskeletal proteins, lamins and actin, and the endonuclease modulator, caspase-activated deoxyribonuclease (CAD) inhibitor (ICAD) [19]. During Fas-mediated apoptosis, the concomitant activation of many other proteins appears to occur. Receptor-interacting protein (RIP), RIP-associated ICH/CED-3-homologous protein with a DD (RAIDD), and procaspase 2 from part of another signaling cascade of the Fas-mediated death pathway were shown to be activated [20]. The activation of the RIP-RAIDD arm of the cell death machinery was demonstrated to serve as a co-stimulator of the FADD-FLICE system [19]. Moreover, upregulation of cytoplasmic DAXX, leading to induction of the stress-activated protein kinase/c-Jun *N*-terminal kinase (SAP/JNK) pathway, represents yet another mechanism by which Fas-mediated apoptosis may occur [21]. The activated form of caspases executes the apoptotic process by cleaving various intracellular substrates leading to genomic DNA fragmentation and resulting in cell membrane blebbing and the exposure of phagocytosis signaling molecules on the cell surface. As mentioned above, FasL-dependent apoptosis plays a critical role in the peripheral elimination of prolongly activated lymphocytes at the end of an immune response [22,23]. Thus, it may be true that FasL has a central role in many of the biological phenomena of activation-induced T-cell apoptosis. In fact, *gld* mice that carry hereditary mutations in the genes encoding FasL are found to suffer from accumulating lymphocytes and a lethal enlargement of lymph nodes. These findings indicate that the main biological role of FasL is to signal the Fas^+ cells to induce instructive apoptosis during the peripheral elimination of lymphocytes. FasL is also expressed in immuno-privileged tissue in which it is difficult to elicit an inflammatory response such as testis and eye [24,25]. FasL may also act as a barrier in the vessel [26]. Significant expression was found on vascular endothelial cells, where it may prevent leukocyte exfiltration into non-inflamed tissues, again by triggering the apoptosis of Fas-expressing leukocytes [27].

TNF, first identified in 1975, is a conventional cytokine and representative of a large superfamily of cytokines that exert physiological roles in cell proliferation, cell death and inflammation as well

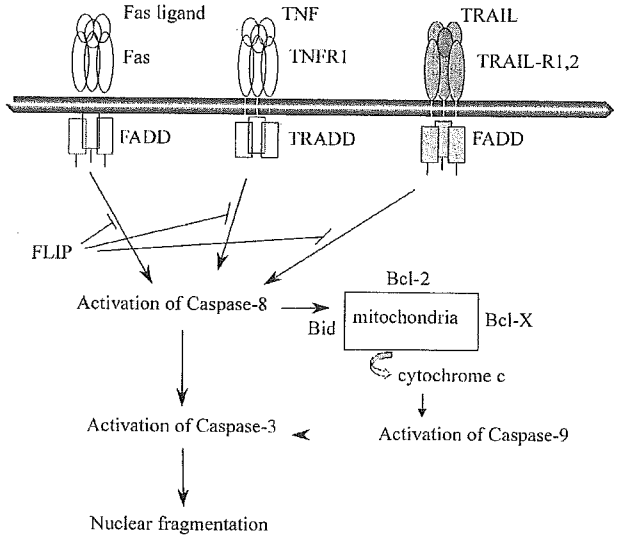

Figure 3. The death ligand-mediated apoptotic pathway. Ligation of the death ligand receptor leads to the formation of DISC comprising the adaptor protein (FADD, TRADD) and procaspase-8 and resulting in the activation of caspase-8. The binding of FLIP to FADD inhibits caspase-8 activation. Caspase-8 can then either directly activate effector caspases (caspase-3) or cleave the proapoptotic Bcl-2 family member Bid. Bid acts with the proapoptotic Bcl-2 family. The involvement of the mitochondria is manifested by the release of cytochrome c into the cytosol where it associates with Apaf-1 and procaspase-9 to form the apoptosome, leading to caspase-9 activation and subsequent caspase-3 activation and nuclear fragmentation

as pathological roles in immunological processes. The best-characterised death receptor is TNFR1. Trimerised TNFR1 can recruit an adaptor molecule, TNFR-associated DD (TRADD), which subsequently recruits FADD and procaspase-8. The intracellular signaling cascade through TNFR1 seems to be more complex than that through Fas. Indeed, in addition to recruiting caspase-activating adaptor molecules, TNFR1 induces the recruitment of many other proteins that engage various signal transduction pathways, some of which either abrogate or potentiate the apoptotic response. For example, TRADD also binds serine-threonine kinase RIP, thereby coupling the stimulation of TNFR1 to the activation of nuclear factor-κB (NF-κB) and offering protection against TNF-induced apoptosis [28]. RIP possesses a functional *N*-terminal kinase domain and can autophosphorylate itself, but this phospharylation does not induce activation of NF-κB. TNF receptor-associated factor 2 (TRAF2) has been likewise implicated in the activation of NF-κB through stimulation of NF-κB-inducing kinase (NIK). However, studies TRAF-2-knockout mice indicated that RIP is most likely responsible for the activation of NF-κB, whereas TRAF2 preferentially activates JNK. TNF knockout mice exhibited increased susceptibility to microbial infection and suppressed inflammatory response when challenged with bacterial endotoxin. These findings together with results obtained *in vitro* suggested that the main biological role of TNF is the induction of inflammatory-response and stress-response genes through the transcription factors AP-1 and NF-κB.

TRAIL was first identified in 1995 based on its sequence homology to other members of the TNF superfamily [29]. TRAIL is also a type 2 transmembrane protein and its highest level of homology is with FasL, exhibiting 28% amino acid identity in the extracellular receptor-binding motif. Two other unique characteristics of TRAIL have been identified. First, TRAIL selectively induces apoptosis both *in vitro* in transformed cells and *in vivo* in tumor cells but not in most normal cells, except thymocytes, neural cells and hepatocytes [30–32]. Second, whereas the expression of other members of the TNF family is tightly regulated and often only transiently induced on activated cells, the transcript of TRAIL was constitutively expressed in some tissues including spleen, lung and prostate [29]. Because the level of TRAIL expression is not consistent with numbers of apoptotic cells, it was assumed that the expression of its cognate receptor would be restricted or alternatively, that apoptosis in only limited cells would be induced under some biological conditions. However, the regulation of TRAIL-induced cell death appears to be more complex than initially thought because five receptors for TRAIL have been identified including two death-inducing receptors (DR4 and DR5), two decoy receptors (DcR1 and DcR2) [33,34], and the secreted TNFR homologue receptor osteoprotegerin [35,36]. The cytoplasmic region of two of these receptors, DR4 and DR5, contains a region with significant homology to the DD of TNFR1 and Fas, and it was confirmed that DR4 and DR5 are able to induce signals for apoptosis [37]. By contrast, DcR2 contains an incomplete DD and so is unable to transduce a death signal [38]. Similarly, DcR1, which unlike the others lacks a cytoplasmic domain and is bound to the cell surface via a glycosyl-phosphatidylinositol (GPI) anchor, does not mediate apoptosis upon ligation [39]. The

activation of caspase has been demonstrated in TRAIL-induced apoptosis *in vitro*. Many of the same caspases involved in Fas and TNF-induced apoptosis were shown to participate in the TRAIL-induced cell death. The activation of death-induced TRAIL-receptors (DR4 and DR5) initiates recruitment of FADD, which in turn directly recruits procaspase-8 to form DISC and results in autoactivation of caspase-8, which then activates downstream effector caspases or the cleaved RIP directly [40]. The NF-κB or JNK signaling pathway was also shown to be activated through DR4 and DR5, respectively, analogous to TNFR1 [41]. It has been suggested that decoy receptors operate to protect normal cells from TRAIL-mediated apoptosis [33,38]. Also, certain intracellular regulatory molecules that control TRAIL-induced apoptosis, such as cFLIP (cellular-FLICE-inhibitory protein), may also operate [42]. Early studies indicated a high level of cFLIP in a TRAIL-resistant melanoma cell line [43]. Furthermore, the level of cFLIP clearly correlated with the sensitivity to TRAIL in some keratinocytes [42]. In addition, it was shown that overexpression of cFLIP frequently causes cells to become resistant to TRAIL because in the presence of cFLIP, procaspase-8 is unable to convert processed caspase-8 generated at the DISC and so remains inactivated [44]. However, inhibition of overall transcription and translation was observed in TRAIL-induced apoptosis without a change in cFLIP levels [45]. These results suggest a significant role for cFLIP in modulating the sensitivity to TRAIL of many cells. It was recently reported that mice deficient in TRAIL exhibit defects of apoptosis in the thymus and develop heightened autoimmune responses, hypersensitivity, to collagen-induced arthritis and streptozotocin-induced diabetes [46]. However, the physiological defect was slighter in the TRAIL-deficient mice than either the FasL- or TNF-deficient mice. Thus, TRAIL seems to have minor physiological roles.

The screening of an EST database revealed another death ligand, called TWEAK [47], whose closest homologue is TNF. Like TNF, TWEAK efficiently promotes apoptosis in certain tumor cell lines and the inhibition of protein synthesis in TWEAK-induced cells further augments apoptosis. TWEAK efficiently activates NF-κB and induces expression of IL-8. Unlike TNF, whose expression is found in activated lymphoid and endothelial cells, the TWEAK transcript was found to be constitutively expressed in many tissues. DR3 was originally identified as a molecule interacting with TNFR1 and reported to be a receptor for TWEAK [48,49]. Similar to TNF-TNFR1 signaling, the activation of DR3 was demonstrated to induce apoptosis as well as the activation of NF-κB and the apoptosis is mediated via interactions with TRADD, FADD and caspase 8, while the activation of NF-κB is induced by a TRADD, TRAF2 and RIP-mediated pathway. However, a high level of TWEAK expression was found in many tissues, whereas DR3 expression was demonstrated to be restricted to peripheral blood lymphocytes (PBLs), thymus, spleen, colon and small intestine [50]. The physiological role of TWEAK remains to be elucidated.

HIV INFECTION AND DEATH LIGANDS

Extensive death ligand-mediated apoptosis is thought to occur in many infectious diseases. Significant augmentation of FasL expression is found in cells expressing hepatitis B and hepatitis C viruses [51,52], although some studies indicated that an increased level of FasL *in vivo* is not associated with HIV disease progression [53,54]. It is remarkable that HIV-1-infected T cells in culture as well as T cells from HIV-infected individuals are highly susceptible to Fas-induced apoptosis [55]. Clinical studies have shown that the expression of Fas as well as the susceptibility to Fas-induced apoptosis increased significantly in cultured $CD4^+$ and $CD8^+$ T cells derived from HIV-1-infected individuals and this high level of Fas expression was positively correlated with disease progression [56]. An increased level of soluble Fas was also found in the plasma of HIV-1-infected individuals and this can be used as a marker for the prognosis of AIDS [57]. FasL was also shown to be upregulated in cultured $CD4^+$ and $CD8^+$ T cells from AIDS patients and, a high level of soluble FasL in serum was found in AIDS patients. Furthermore, FasL expression on macrophages was detected in lymphoid tissue of HIV-1-infected subjects [58]. The observation that retinoic acid inhibits the expression of FasL and the subsequent apoptosis of $CD4^+$ T cells *ex vivo* further supports a causal role for Fas-FasL interactions in the $CD4^+$ T cell death that is induced by HIV infection [59]. Interestingly, the exposure of uninfected monocytes to HIV-1 particles *in vitro* has been

reported to enhance significantly FasL expression, suggesting that HIV-1 can induce Fas-dependent apoptosis through the interaction of monocytes with T cells [60,61]. Furthermore, the crosslinking of the CD4 molecule with HIV-1 gp120 on $CD4^+$ T cells activates the Fas-FasL pathway and Nef-expressing T cells co-express FasL, thereby becoming potential killer cells of uninfected Fas-expressing T cells [62,63]. Similarly, Tat, which is secreted by HIV-infected cells, was shown to upregulate Fas and FasL expression on uninfected cells and enhance their susceptibility to Fas-induced apoptosis [61,64]. Since it is known to be expressed even before integration, Nef may protect infected cells from apoptosis and permit infection in resting cells. Interestingly, significant protection against apoptosis is provided through the downregulation of ASK-1 signaling by Fas-FasL suggesting that Nef acts as an anti-apoptotic protein in the infected cells during its replication [65]. It is also clear that Vpu enhances susceptibility to Fas-induced apoptosis [66]. However, the possible involvement of the Fas/FasL pathway in AICD of $CD4^+$ T cells from HIV-1-infected individuals [67,68] remains controversial. Katsikis *et al.* reported that the AICD cultured $CD4^+$ T cells from HIV-infected patients was Fas-independent [69] and it was shown that neither Fas protein nor biologically active FasL was detectable at significant levels in freshly isolated T cells from HIV-1-infected individuals [54]. In addition, FasL-mediated apoptosis may contribute to the elimination of virus-infected cells by the virus-specific cytotoxic lymphocytes or NK cells [70,71].

Susceptibility to TNF in $CD4^+$ T cells isolated from HIV-infected individuals has also been investigated extensively. Although an early report found that peripheral blood T cells from HIV-positive patients were resistant to apoptosis that was induced by ligation of TNFR [56], a more recent study showed that both $CD4^+$ and $CD8^+$ T cells from HIV-infected individuals were significantly susceptible to TNFR1- and R2-induced apoptosis [72]. The possible contribution of TNFR-mediated apoptosis to $CD8^+$ T cell depletion was implied from the observation that ligation of Env to the CXCR4 coreceptor upregulated the expression of TNFR2 on $CD8^+$ T cells, which became susceptible to death induced by the membrane-bound form of TNF expressed on macrophages [73]. An increased level of TNF was also detected in the serum of symptomatic individuals and clearly high levels of soluble TNFR2 were found to be predictive of HIV disease progression [74].

HIV INFECTION AND TRAIL

Treatment with interferon (IFN) significantly augmented the expression of TRAIL on $CD4^+$ T cells [75], monocytes [76] and dendritic cells (DC) [77]. In addition, infection with measles virus augmented TRAIL expression on DC [78]. Therefore, it is possible that TRAIL is involved in the pathogenesis of HIV. In fact, TRAIL, but not FasL-dependent AICD, was detected in $CD4^+$ T cells isolated from HIV-1-infected individuals *in vitro* [79,80]. TRAIL might contribute to a constructive apoptosis of virus-infected cells because T cells from HIV-1-infected patients were more susceptible to the induction of apoptosis by this ligand than uninfected cells, suggesting that TRAIL is involved in HIV-associated T-cell apoptosis [79]. In fact, AICD in $CD4^+$ T cells isolated from HIV-1-infected individuals was inhibited by antagonistic TRAIL-specific antibodies [80]. Furthermore, using an HIV-1-infected mouse model, a significant level of TRAIL-dependent apoptosis in uninfected $CD4^+$ T cells was found. The spleen tissue of hu-PBL-NOD-SCID mice was investigated following infection with HIV-1 and large numbers of $TUNEL^+$ $CD4^+$ cells were found mainly in uninfected cells. The number of $TUNEL^+$ cells was clearly inhibited after administration of anti-TRAIL but not anti-FasL antibody, suggesting that TRAIL is a major death ligand in HIV-1-infected tissues [81,82]. Following infection with HIV-1, Tat protein is released by macrophages or monocytes and seems to upregulate the expression of TRAIL on macrophages as shown by Zhang, indicating that TRAIL-dependent cell death occurs in bystander $CD4^+$ T cells, perhaps triggered by Tat produced from HIV-1-infected cells [83,84].

It is likely that TRAIL is primarily responsible for the apoptosis of bystander $CD4^+$ T cells in HIV-infected lymphoid organs. However, several issues remain to be resolved. First, the mechanism by which HIV-1 infection induces the expression of TRAIL in $CD4^+$ T cells remains to be determined. It was found that the number of $TRAIL^+$ cells was consistently higher in HIV-1-infected mice than uninfected mice. A similar upregulation of TRAIL expression with HIV-1 infection was observed especially on HIV-1-infected

macrophages [85]. The expression of TRAIL on T cells is induced by a variety of stimuli, including type I IFNs and TCR-mediated signals [75,86,87]. Thus it can be postulated that TRAIL was induced to express on HIV-1-uninfected $CD4^+$ T cells by viral or cellular factors from either HIV-1-infected or bystander cells in HIV-1-infected lymphoid organs. Second, it is necessary to determine the receptor molecule involved in TRAIL-mediated apoptosis. It is not yet clear which receptor contributes to this phenomenon. In other viral infections, viral proteins regulate the expression of these receptors. In adenovirus, E3 downregulates its receptor DR4 and DR5 [88]. In respiratory syncytial virus, infection strongly upregulated DR4 and DR5 expression [89]. In HIV infection, Tat and gp120 seem to upregulate DR4 and DR5 expression.

TRAIL seems to be one of the most significant molecules in HIV infection [81,85,90]. This ligand was predominantly expressed on macrophages and monocytes after HIV-1 infection, and was able to induce apoptosis in neurons *in vitro* and *in vivo*, which might explain the neuronal death in HIV-encephalopathy. Recently, a murine model of HIV-encephalopathy was developed and it was found that neuronal apoptosis was significantly induced by TRAIL expressed on HIV-infected macrophages [85]. Furthermore, neuronal apoptosis was confirmed in the brain tissue of HIV-1-encephalopathy patients and cells cultured *in vitro* [90,91]. It is possible that TRAIL has a central role in disease progression in some virus-induced diseases.

CONCLUSION

Although the mechanism of the apoptosis in HIV-infected individuals is likely to be multifactorial, its induction is a critical event *in vivo*. The death ligands in HIV infection are important for this apoptosis in addition to mitochondria-mediated apoptosis. A novel immune-based therapy for modulating the apoptosis in HIV infection is awaited.

ACKNOWLEDGEMENTS

The authors thanks the many scientists who have helped with their work over the years, especially N. Yamamoto and H. Mizusawa for discussions. Research in the authors' laboratory is supported by grants from the Ministry of Health, Labor, and Welfare and the Ministry of Education, Culture, Sports, Science, and Technology of Japan.

REFERENCES

1. Badley AD, Roumier T, Lum JJ, *et al.* Mitochondrion-mediated apoptosis in HIV-1 infection. *Trends Pharmacol Sci* 2003; **24**: 298–305.
2. Arnoult D, Petit F, Lelievre JD, *et al.* Mitochondria in HIV-1-induced apoptosis. *Biochem Biophys Res Commun* 2003; **304**: 561–574.
3. Lifson JD, Reyes GR, McGrath MS, *et al.* AIDS retrovirus induced cytopathology: giant cell formation and involvement of CD4 antigen. *Science* 1986; **232**: 1123–1127.
4. Terai C, Kornbluth RS, Pauza CD, *et al.* Apoptosis as a mechanism of cell death in cultured T lymphoblasts acutely infected with HIV-1. *J Clin Invest* 1991; **87**: 1710–1715.
5. Rinfret A, Latendresse H, Lefebvre R, *et al.* Human immunodeficiency virus-infected multinucleated histiocytes in oropharyngeal lymphoid tissues from two asymptomatic patients. *Am J Pathol* 1991; **138**: 421–426.
6. Frankel SS, Wenig BM, Burke AP, *et al.* Replication of HIV-1 in dendritic cell-derived syncytia at the mucosal surface of the adenoid. *Science* 1996; **272**: 115–117.
7. Sodroski J, Goh WC, Rosen C, *et al.* Role of the HTLV-III/LAV envelope in syncytium formation and cytopathicity. *Nature* 1986; **322**: 470–474.
8. Ferri KF, Jacotot E, Blanco J, *et al.* Apoptosis control in syncytia induced by the HIV type 1-envelope glycoprotein complex: role of mitochondria and caspases. *J Exp Med* 2000; **192**: 1081–1092.
9. Castedo M, Roumier T, Blanco J, *et al.* Sequential involvement of Cdk1, mTOR and p53 in apoptosis induced by the HIV-1 envelope. *EMBO J* 2002; **21**: 4070–4080.
10. Sastry KJ, Marin MC, Nehete PN, *et al.* Expression of human immunodeficiency virus type I tat results in down-regulation of bcl-2 and induction of apoptosis in hematopoietic cells. *Oncogene* 1996; **13**: 487–493.
11. Bartz SR, Emerman M. Human immunodeficiency virus type 1 Tat induces apoptosis and increases sensitivity to apoptotic signals by up-regulating FLICE/caspase-8. *J Virol* 1999; **73**: 1956–1963.
12. Jacotot E, Ravagnan L, Loeffler M, *et al.* The HIV-1 viral protein R induces apoptosis via a direct effect on the mitochondrial permeability transition pore. *J Exp Med* 2000; **191**: 33–46.
13. Green DR, Droin N, Pinkoski M. Activation-induced cell death in T cells. *Immunol Rev* 2003; **193**: 70–81.
14. Muro-Cacho CA, Pantaleo G, Fauci AS. Analysis of apoptosis in lymph nodes of HIV-infected persons. Intensity of apoptosis correlates with the general state of activation of the lymphoid tissue and not

with stage of disease or viral burden. *J Immunol* 1995; **154**: 5555–5566.
15. Finkel TH, Tudor-Williams G, Banda NK, *et al.* Apoptosis occurs predominantly in bystander cells and not in productively infected cells of HIV- and SIV-infected lymph nodes. *Nat Med* 1995; **1**: 129–134.
16. Suda T, Takahashi T, Golstein P, *et al.* Molecular cloning and expression of the Fas ligand, a novel member of the tumor necrosis factor family. *Cell* 1993; **75**: 1169–1178.
17. Medema JP, Scaffidi C, Kischkel FC, *et al.* FLICE is activated by association with the CD95 death-inducing signaling complex (DISC). *EMBO J* 1997; **16**: 2794–2804.
18. Medema JP, Toes RE, Scaffidi C, *et al.* Cleavage of FLICE (caspase-8) by granzyme B during cytotoxic T lymphocyte-induced apoptosis. *Eur J Immunol* 1997; **27**: 3492–3498.
19. Cohen GM. Caspases: the executioners of apoptosis. *Biochem J* 1997; **326**: 1–16.
20. Duan H, Dixit VM. RAIDD is a new 'death' adaptor molecule. *Nature* 1997; **385**: 86–89.
21. Yang X, Khosravi-Far R, Chang HY, *et al.* Daxx, a novel Fas-binding protein that activates JNK and apoptosis. *Cell* 1997; **89**: 1067–1076.
22. Sharma K, Wang RX, Zhang LY, *et al.* Death the Fas way: regulation and pathophysiology of CD95 and its ligand. *Pharmacol Ther* 2000; **88**: 333–347.
23. Newell MK, Desbarats J. Fas ligand: receptor or ligand? *Apoptosis* 1999; **4**: 311–315.
24. Bellgrau D, Gold D, Selawry H, *et al.* A role for CD95 ligand in preventing graft rejection. *Nature* 1995; **377**: 630–632.
25. Griffith TS, Brunner T, Fletcher SM, *et al.* Fas ligand-induced apoptosis as a mechanism of immune privilege. *Science* 1995; **270**: 1189–1192.
26. Walsh K, Sata M. Negative regulation of inflammation by Fas ligand expression on the vascular endothelium. *Trends Cardiovasc Med* 1999; **9**: 34–41.
27. Liles WC, Kiener PA, Ledbetter JA, *et al.* Differential expression of Fas (CD95) and Fas ligand on normal human phagocytes: implications for the regulation of apoptosis in neutrophils. *J Exp Med* 1996; **184**: 429–440.
28. Hsu H, Xiong J, Goeddel DV. The TNF receptor 1-associated protein TRADD signals cell death and NF-kappa B activation. *Cell* 1995; **81**: 495–504.
29. Wiley SR, Schooley K, Smolak PJ, *et al.* Identification and characterization of a new member of the TNF family that induces apoptosis. *Immunity* 1995; **3**: 673–682.
30. Cretney E, Uldrich AP, Berzins SP, *et al.* Normal thymocyte negative selection in TRAIL-deficient mice. *J Exp Med* 2003; **198**: 491–496.
31. Nitsch R, Bechmann I, Deisz RA, *et al.* Human brain-cell death induced by tumour-necrosis-factor-related apoptosis-inducing ligand (TRAIL). *Lancet* 2000; **356**: 827–828.
32. Mori E, Thomas M, Motoki K, *et al.* Human normal hepatocytes are susceptible to apoptosis signal mediated by both TRAIL-R1 and TRAIL-R2. *Cell Death Differ* 2004; **11**: 203–207.
33. Pan G, Ni J, Wei YF, *et al.* An antagonist decoy receptor and a death domain-containing receptor for TRAIL. *Science* 1997; **277**: 815–818.
34. Walczak H, Degli-Esposti MA, Johnson RS, *et al.* TRAIL-R2: a novel apoptosis-mediating receptor for TRAIL. *EMBO J* 1997; **16**: 5386–5397.
35. Almasan A, Ashkenazi A. Apo2L/TRAIL: apoptosis signaling, biology, and potential for cancer therapy. *Cytokine Growth Factor Rev* 2003; **14**: 337–348.
36. MacFarlane M. TRAIL-induced signalling and apoptosis. *Toxicol Lett* 2003; **139**: 89–97.
37. Pan G, O'Rourke K, Chinnaiyan AM, *et al.* The receptor for the cytotoxic ligand TRAIL. *Science* 1997; **276**: 111–113.
38. Sheridan JP, Marsters SA, Pitti RM, *et al.* Control of TRAIL-induced apoptosis by a family of signaling and decoy receptors. *Science* 1997; **277**: 818–821.
39. Legembre P, Moreau P, Daburon S, *et al.* Potentiation of Fas-mediated apoptosis by an engineered glycosylphosphatidylinositol-linked Fas. *Cell Death Differ* 2002; **9**: 329–339.
40. Kischkel FC, Lawrence DA, Chuntharapai A, *et al.* Apo2L/TRAIL-dependent recruitment of endogenous FADD and caspase-8 to death receptors 4 and 5. *Immunity* 2000; **12**: 611–620.
41. Lin Y, Devin A, Cook A, *et al.* The death domain kinase RIP is essential for TRAIL (Apo2L)-induced activation of IkappaB kinase and c-Jun *N*-terminal kinase. *Mol Cell Biol* 2000; **20**: 6638–6645.
42. Leverkus M, Neumann M, Mengling T, *et al.* Regulation of tumor necrosis factor-related apoptosis-inducing ligand sensitivity in primary and transformed human keratinocytes. *Cancer Res* 2000; **60**: 553–559.
43. Griffith TS, Chin WA, Jackson GC, *et al.* Intracellular regulation of TRAIL-induced apoptosis in human melanoma cells. *J Immunol* 1998; **161**: 2833–2840.
44. MacFarlane M, Harper N, Snowden RT, *et al.* Mechanisms of resistance to TRAIL-induced apoptosis in primary B cell chronic lymphocytic leukaemia. *Oncogene* 2002; **21**: 6809–6818.
45. Ahmad M, Shi Y. TRAIL-induced apoptosis of thyroid cancer cells: potential for therapeutic intervention. *Oncogene* 2000; **19**: 3363–3371.
46. Lamhamedi-Cherradi SE, Zheng SJ, Maguschak KA, *et al.* Defective thymocyte apoptosis and accelerated autoimmune diseases in TRAIL-/- mice. *Nat Immunol* 2003; **4**: 255–260.

47. Chicheportiche Y, Bourdon PR, Xu H, *et al.* TWEAK, a new secreted ligand in the tumor necrosis factor family that weakly induces apoptosis. *J Biol Chem* 1997; **272**: 32401–32410.
48. Kitson J, Raven T, Jiang YP, *et al.* A death-domain-containing receptor that mediates apoptosis. *Nature* 1996; **384**: 372–375.
49. Marsters SA, Sheridan JP, Pitti RM, *et al.* Identification of a ligand for the death-domain-containing receptor Apo3. *Curr Biol* 1998; **8**: 525–528.
50. Chinnaiyan AM, O'Rourke K, Yu GL, *et al.* Signal transduction by DR3, a death domain-containing receptor related to TNFR-1 and CD95. *Science* 1996; **274**: 990–992.
51. Yoo YG, Lee MO. Hepatitis B virus X protein induces expression of Fas ligand gene through enhancing transcriptional activity of early growth response factor. *J Biol Chem* 2004; **279**: 36242–36249.
52. Ruggieri A, Murdolo M, Rapicetta M. Induction of FAS ligand expression in a human hepatoblastoma cell line by HCV core protein. *Virus Res* 2003; **97**: 103–110.
53. Vasilescu A, Heath SC, Diop G, *et al.* Genomic analysis of Fas and FasL genes and absence of correlation with disease progression in AIDS. *Immunogenetics* 2004; **56**: 56–60.
54. Sieg S, Smith D, Yildirim Z, *et al.* Fas ligand deficiency in HIV disease. *Proc Natl Acad Sci USA* 1997; **94**: 5860–5865.
55. Ohnimus H, Heinkelein M, Jassoy C. Apoptotic cell death upon contact of CD4+ T lymphocytes with HIV glycoprotein-expressing cells is mediated by caspases but bypasses CD95 (Fas/Apo-1) and TNF receptor 1. *J Immunol* 1997; **159**: 5246–5252.
56. Katsikis PD, Wunderlich ES, Smith CA, *et al.* Fas antigen stimulation induces marked apoptosis of T lymphocytes in human immunodeficiency virus-infected individuals. *J Exp Med* 1995; **181**: 2029–2036.
57. Medrano FJ, Leal M, Arienti D, *et al.* Tumor necrosis factor beta and soluble APO-1/Fas independently predict progression to AIDS in HIV-seropositive patients. *AIDS Res Hum Retroviruses* 1998; **14**: 835–843.
58. Dockrell DH, Badley AD, Villacian JS, *et al.* The expression of Fas Ligand by macrophages and its upregulation by human immunodeficiency virus infection. *J Clin Invest* 1998; **101**: 2394–2405.
59. Yang Y, Bailey J, Vacchio MS, *et al.* Retinoic acid inhibition of *ex vivo* human immunodeficiency virus-associated apoptosis of peripheral blood cells. *Proc Natl Acad Sci USA* 1995; **92**: 3051–3055.
60. Badley AD, McElhinny JA, Leibson PJ, *et al.* Upregulation of Fas ligand expression by human immunodeficiency virus in human macrophages mediates apoptosis of uninfected T lymphocytes. *J Virol* 1996; **70**: 199–206.
61. Westendorp MO, Frank R, Ochsenbauer C, *et al.* Sensitization of T cells to CD95-mediated apoptosis by HIV-1 Tat and gp120. *Nature* 1995; **375**: 497–500.
62. Banda NK, Bernier J, Kurahara DK, *et al.* Crosslinking CD4 by human immunodeficiency virus gp120 primes T cells for activation-induced apoptosis. *J Exp Med* 1992; **176**: 1099–1106.
63. Zauli G, Gibellini D, Secchiero P, *et al.* Human immunodeficiency virus type 1 Nef protein sensitizes CD4(+) T lymphoid cells to apoptosis via functional upregulation of the CD95/CD95 ligand pathway. *Blood* 1999; **93**: 1000–1010.
64. Li CJ, Friedman DJ, Wang C, *et al.* Induction of apoptosis in uninfected lymphocytes by HIV-1 Tat protein. *Science* 1995; **268**: 429–431.
65. Geleziunas R, Xu W, Takeda K, *et al.* HIV-1 Nef inhibits ASK1-dependent death signalling providing a potential mechanism for protecting the infected host cell. *Nature* 2001; **410**: 834–838.
66. Casella CR, Rapaport EL, Finkel TH. Vpu increases susceptibility of human immunodeficiency virus type 1-infected cells to fas killing. *J Virol* 1999; **73**: 92–100.
67. Baumler CB, Bohler T, Herr I, *et al.* Activation of the CD95 (APO-1/Fas) system in T cells from human immunodeficiency virus type-1-infected children. *Blood* 1996; **88**: 1741–1746.
68. Estaquier J, Tanaka M, Suda T, *et al.* Fas-mediated apoptosis of CD4+ and CD8+ T cells from human immunodeficiency virus-infected persons: differential *in vitro* preventive effect of cytokines and protease antagonists. *Blood* 1996; **87**: 4959–4966.
69. Katsikis PD, Garcia-Ojeda ME, Wunderlich ES, *et al.* Activation-induced peripheral blood T cell apoptosis is Fas independent in HIV-infected individuals. *Int Immunol* 1996; **8**: 1311–1317.
70. Petrovas C, Mueller YM, Katsikis PD. HIV-specific CD8+ T cells: serial killers condemned to die? *Curr HIV Res* 2004; **2**: 153–162.
71. Lum JJ, Schnepple DJ, Nie Z, *et al.* Differential effects of interleukin-7 and interleukin-15 on NK cell anti-human immunodeficiency virus activity. *J Virol* 2004; **78**: 6033–6042.
72. de Oliveira Pinto LM, Garcia S, Lecoeur H, *et al.* Increased sensitivity of T lymphocytes to tumor necrosis factor receptor 1 (TNFR1)- and TNFR2-mediated apoptosis in HIV infection: relation to expression of Bcl-2 and active caspase-8 and caspase-3. *Blood* 2002; **99**: 1666–1675.
73. Herbein G, Mahlknecht U, Batliwalla F, *et al.* Apoptosis of CD8+ T cells is mediated by macrophages through interaction of HIV gp120 with chemokine receptor CXCR4. *Nature* 1998; **395**: 189–194.

74. Zangerle R, Gallati H, Sarcletti M, *et al.* Tumor necrosis factor alpha and soluble tumor necrosis factor receptors in individuals with human immunodeficiency virus infection. *Immunol Lett* 1994; **41**: 229–234.
75. Kayagaki N, Yamaguchi N, Nakayama M, *et al.* Type I interferons (IFNs) regulate tumor necrosis factor-related apoptosis-inducing ligand (TRAIL) expression on human T cells: a novel mechanism for the antitumor effects of type I IFNs. *J Exp Med* 1999; **189**: 1451–1460.
76. Griffith TS, Wiley SR, Kubin MZ, *et al.* Monocyte-mediated tumoricidal activity via the tumor necrosis factor-related cytokine, TRAIL. *J Exp Med* 1999; **189**: 1343–1354.
77. Sedger LM, Shows DM, Blanton RA, *et al.* IFN-gamma mediates a novel antiviral activity through dynamic modulation of TRAIL and TRAIL receptor expression. *J Immunol* 1999; **163**: 920–926.
78. Vidalain PO, Azocar O, Lamouille B, *et al.* Measles virus induces functional TRAIL production by human dendritic cells. *J Virol* 2000; **74**: 556–559.
79. Jeremias I, Herr I, Boehler T, *et al.* TRAIL/Apo-2-ligand-induced apoptosis in human T cells. *Eur J Immunol* 1998; **28**: 143–152.
80. Katsikis PD, Garcia-Ojeda ME, Torres-Roca JF, *et al.* Interleukin-1 beta converting enzyme-like protease involvement in Fas-induced and activation-induced peripheral blood T cell apoptosis in HIV infection. TNF-related apoptosis-inducing ligand can mediate activation-induced T cell death in HIV infection. *J Exp Med* 1997; **186**: 1365–1372.
81. Miura Y, Misawa N, Maeda N, *et al.* Critical contribution of tumor necrosis factor-related apoptosis-inducing ligand (TRAIL) to apoptosis of human CD4+ T cells in HIV-1-infected hu-PBL-NOD-SCID mice. *J Exp Med* 2001; **193**: 651–660.
82. Lum JJ, Pilon AA, Sanchez-Dardon J, *et al.* Induction of cell death in human immunodeficiency virus-infected macrophages and resting memory CD4 T cells by TRAIL/Apo2l. *J Virol* 2001; **75**: 11128–11136.
83. Zhang M, Li X, Pang X, *et al.* Identification of a potential HIV-induced source of bystander-mediated apoptosis in T cells: upregulation of trail in primary human macrophages by HIV-1 tat. *J Biomed Sci* 2001; **8**: 290–296.
84. Yang Y, Tikhonov I, Ruckwardt TJ, *et al.* Monocytes treated with human immunodeficiency virus Tat kill uninfected CD4(+) cells by a tumor necrosis factor-related apoptosis-induced ligand-mediated mechanism. *J Virol* 2003; **77**: 6700–6708.
85. Miura Y, Koyanagi Y, Mizusawa H. TNF-related apoptosis-inducing ligand (TRAIL) induces neuronal apoptosis in HIV-encephalopathy. *J Med Dent Sci* 2003; **50**: 17–25.
86. Martinez-Lorenzo MJ, Anel A, Gamen S, *et al.* Activated human T cells release bioactive Fas ligand and APO2 ligand in microvesicles. *J Immunol* 1999; **163**: 1274–1281.
87. Musgrave BL, Phu T, Butler JJ, *et al.* Murine TRAIL (TNF-related apoptosis inducing ligand) expression induced by T cell activation is blocked by rapamycin, cyclosporin A, and inhibitors of phosphatidylinositol 3-kinase, protein kinase C, and protein tyrosine kinases: evidence for TRAIL induction via the T cell receptor signaling pathway. *Exp Cell Res* 1999; **252**: 96–103.
88. Tollefson AE, Toth K, Doronin K, *et al.* Inhibition of TRAIL-induced apoptosis and forced internalization of TRAIL receptor 1 by adenovirus proteins. *J Virol* 2001; **75**: 8875–8887.
89. Kotelkin A, Prikhod'ko EA, Cohen JI, *et al.* Respiratory syncytial virus infection sensitizes cells to apoptosis mediated by tumor necrosis factor-related apoptosis-inducing ligand. *J Virol* 2003; **77**: 9156–9172.
90. Miura Y, Misawa N, Kawano Y, *et al.* Tumor necrosis factor-related apoptosis-inducing ligand induces neuronal death in a murine model of HIV central nervous system infection. *Proc Natl Acad Sci USA* 2003; **100**: 2777–2782.
91. Ryan LA, Peng H, Erichsen DA, *et al.* TNF-related apoptosis-inducing ligand mediates human neuronal apoptosis: links to HIV-1-associated dementia. *J Neuroimmunol* 2004; **148**: 127–139.

Human Reproduction Vol.20, No.6 pp. 1477–1484, 2005
Advance Access publication February 25, 2005
doi:10.1093/humrep/deh783

Reproduction of menstrual changes in transplanted human endometrial tissue in immunodeficient mice

Rui Matsuura-Sawada[1,4], Takashi Murakami[1], Yuka Ozawa[1], Hiroshi Nabeshima[1], Jun-ichi Akahira[1], Yumi Sato[1], Yoshio Koyanagi[2], Mamoru Ito[3], Yukihiro Terada[1] and Kunihiro Okamura[1]

[1]Tohoku University Graduate School of Medicine – Obstetrics and Gynecology, Seiryo-machi1-1, Aoba-ku, Sendai Japan, [2]Virus Research, Kyoto University – Laboratory of Viral Pathogenesis, Kyoto and [3]Central Institute for Experimental Animals, Kawasaki, Japan

[4]To whom correspondence should be addressed. E-mail: sawada@ob-gy.med.tohoku.ac.jp

BACKGROUND: Cultures of human endometrial tissue are useful for analysing the mechanisms underlying the menstrual cycle. However, long-term culture of endometrial tissue is difficult *in vitro*. Xenotransplantation of normal human endometrial tissue into immunodeficient mice could allow prolonged survival of the transplanted tissues. METHODS: Proliferative-phase endometrial tissue samples from three women were transplanted into the subcutaneous space of ovariectomized, immunodeficient, non-obese diabetic (NOD)/severe combined immunodeficiency (SCID)/γC^{null} (NOG) mice. The mice were treated with 17β-estradiol (E_2) for the first 14 days after transplantation, followed by E_2 plus progesterone for the next 14 days. The transplants were investigated morphologically and immunohistochemically at various times after implantation. RESULTS: The transplanted tissues contained large numbers of small glands, pseudostratification of the nuclei and dense stroma after treatment with E_2 alone. After treatment with E_2 plus progesterone, subnuclear vacuolation, luminal secretion and decidualization of the stroma were observed. When the hormone treatment ceased, tissue destruction occurred and the transplants returned to the proliferative phase. Lymphocytes were identified immunohistochemically: the numbers of CD56-positive and CD16-negative cells increased significantly in the stroma during the late secretory phase (day 28). CONCLUSIONS: Human endometrial tissue transplanted into NOG mice showed similar histological changes to eutopic endometrial tissue during treatment with sex steroid hormones for 1 month. Moreover, lymphocytes were produced in the transplanted human endometrial tissue. This system represents a new experimental model of the human endometrium *in vivo*.

Key words: endometrial transplants/human endometrium/immunodeficient mouse model/menstrual cycle

Introduction

Endometrial tissue undergoes periodic cycles of proliferation, differentiation and degeneration that are precisely controlled by sex steroid hormones produced in the ovaries. If fertilization does not occur during a cycle, the cells of the endometrium degenerate and slough off, and the organ prepares itself for nidation in the next cycle. These tissue dynamics have, so far, been difficult to reproduce in experimental models. Therefore, the exact mechanisms that are responsible for these processes are poorly understood.

In 1908, the earliest comprehensive description of the cyclical histological changes that occur in the human endometrium was published (Hitschmann and Adler, 1908). Subsequently, Noyes and colleagues described several histological features that are still used today as criteria for endometrial dating: gland mitoses, pseudostratification of the nuclei, subnuclear vacuolation, gland secretion, stromal oedema, stromal mitoses, pseudodecidual reactions and leukocytic infiltration (Noyes *et al.*, 1950). Although these histological changes have been used widely in clinical diagnosis, their implications are not yet fully understood.

To understand the mechanisms of reproduction, it is essential to establish experimental models of the endometrium throughout the menstrual cycle. Many experiments have examined the mechanism of action of steroid hormones on the endometrium in laboratory animals (Jensen and Jacobson, 1962; O'Mally *et al.*, 1970; Flickinger *et al.*, 1977). However, in mature mice and rats, the reproductive cycle is only 4 or 5 days long and decidualization does not occur unless it is triggered by implantation or stimulated by pregnancy (Finn *et al.*, 1992). Similarly, natural ovulation does not occur in mature rabbits unless mating has occurred. Menstruation occurs only in a very limited number of species: humans, a few Old World primates and a few bats. However, there are significant differences between, for example, rhesus monkeys and humans, in terms of the changes that occur in the endometrium at

implantation (Heuser *et al.*, 1945) and the distribution of the aortic branches supplying the uterus (Nelson, 1964). The reproductive cycle, biochemical responses and mechanisms of menstruation clearly differ between species. Therefore, the results of studies in laboratory animals have been difficult to apply directly to humans.

There have been several studies of the human endometrium using *in vitro* endometrial stroma and/or glandular cell cultures over the past two decades (Centola *et al.*, 1984; Irwin *et al.*, 1989; Sugawara *et al.*, 1997). Although these studies have produced many interesting findings, they may not accurately reflect the events that occur *in vivo*. Tissue culture is a useful method for biochemical and histological analyses. However, it is difficult to culture human endometrial tissue over long periods of time—bearing in mind the 1-month duration of each menstrual cycle—in order to observe the relationship between the glandular and stromal cells.

On the other hand, there have been many reports of successful transplantation of human tissues into immunodeficient mice. Nude mice, which lack a thymus and cannot generate mature T lymphocytes, were first used as recipients of xenotransplants of human adenocarcinoma of the sigmoid colon (Rygaard and Povlsen, 1969), and severe combined immunodeficiency (SCID) mice, which are deficient in both T and B lymphocytes, were used as a model of human stem-cell engraftment (McCune *et al.*, 1988). Subsequently, non-obese diabetic (NOD)-SCID mice were developed, which have a higher acceptance rate not only for neoplastic tissue but also for tissue from normal human organs. Weissman and colleagues successfully transplanted normal human ovarian cortex tissue into NOD-SCID mice and observed primordial follicle growth (Weissman *et al.*, 1999). In addition, Sato and colleagues detected by immunohistochemistry the expression of steroidogenic enzymes in NOD-SCID mice after transplantation of human ovarian grafts (Sato *et al.*, 2003). However, although these mice lack T and B lymphocytes, they do have some natural killer (NK) cell activity, which might interfere with engraftment efficiency.

Recently, NOD/SCID/γC^{null} (NOG) immunodeficient mice have been developed; these are double homozygotes for the SCID mutation and the interleukin-2 receptor γ-chain (IL-2Rγ) allelic mutation (γc^{null}). NOG mice lack both T and B lymphocytes, and are defective in NK-cell activity. This severe immunodeficiency results in high engraftment efficiency for human haematopoietic stem cells and full lineage differentiation in NOG mice (Ito *et al.*, 2002).

The aims of the present study were to culture human endometrial tissue in NOG mice, and to reproduce menstrual changes by examining their morphological and immunohistochemical features.

Materials and methods

Ethical approval

All procedures for collecting human specimens and all animal experiments were approved by the Ethics Committee of Tohoku University Graduate School of Medicine, Japan.

Animals

Mature female NOG mice aged 7–8 weeks and weighing 20–25 g were obtained from the Central Institute for Experimental Animals (Kawasaki, Japan). The animals were housed in micro-isolator cages in a barrier facility under well controlled, pathogen-free conditions. The monitored ambient temperature was 22 °C and the animals were maintained under a 12-h light/dark cycle. All housing materials were autoclaved before use. The mice were fed laboratory chow and water *ad libitum*.

Human endometrial tissue

Human endometrial tissues at the proliferative phase of the menstrual cycle were obtained from three premenopausal women (aged 35–49 years) who were undergoing hysterectomy as a result of the benign gynaecological disease, myoma uteri, at Tohoku University Hospital, Japan. Informed consent was obtained from each patient. No lesions of endometriosis were found in the abdomen of the patients during surgery. Each of the patients had a regular menstrual cycle, which had reached the early proliferative phase at the time of surgery; this was confirmed by measuring serum concentrations of 17β-estradiol (E_2) and progesterone. A sample of the endometrial tissue was fixed in 10% neutral buffered formalin, embedded in paraffin, and stained with haematoxylin and eosin in order to determine the menstrual phase according to the method of Noyes *et al.* (1950).

Fresh endometrial tissue was collected in cold sterile Dulbecco's phosphate-buffered saline, cut into fragments (diameter 2 mm) with a safety razor blade and washed twice to remove cellular debris.

Transplantation of endometrial fragments into mice

Eighteen NOG mice were placed under NEMBUTAL (Dainippon Pharmaceutical Co., Ltd, Osaka, Japan) anaesthesia by intraperitoneal injection. A small dorsolateral laparotomy was created in the abdomen of each mouse, and a bilateral ovariectomy was performed to prevent the sex hormones of the animals having an effect on the transplanted tissue. After ovariectomy, two fragments of the human endometrial tissue were transplanted into the subcutaneous space of each mouse. The ovariectomy and transplantation procedure was carried out within 3 h of hysterectomy. The treatment with sex hormones was initiated at the time of tissue transplantation. E_2 (FEMIEST; Yakult Honsha Co., Ltd, Tokyo, Japan) was administered to the mice using a transdermal patch, and progesterone (Progehormone; Mochida Pharmaceutical Co., Ltd, Tokyo, Japan) was administered by subcutaneous injection. The FEMIEST patches were cut into 0.64- or 1-cm^2 sections and attached to the backs of the mice in areas from which the fur had been removed. Mice received E_2 alone for the first 14 days (0.64 cm^2 containing 0.2 mg of E_2 for the first 7 days, and 1 cm^2 containing 0.3 mg of E_2 for the following 7 days), and E_2 (0.64 cm^2) plus progesterone (0.5 mg/kg) for the next 14 days. The patches were changed every 3 days. Hormone administration was stopped after the 28-day treatment period. All procedures were performed

under aseptic conditions in a clean-bench environment. The animals were maintained for a maximum of 35 days without antibiotics.

Histological assessment

Mice were sacrificed by removing blood from the heart under ether anaesthesia at 14, 16, 21, 28, 31 or 35 days after transplantation. The implanted endometrial fragments were extracted and fixed in 10% neutral buffered formalin for ~24 h, then embedded in paraffin. Sections (thickness 3 μm) were stained with haematoxylin and eosin for histological identification. Serum samples were measured using an enzyme-linked immunosorbent assay (Cayman Chemical Co., Ann Arbor, MI, USA).

Immunohistochemical analyses

Single immunohistochemical labelling. Immunohistochemical analyses were performed in order to demonstrate proliferative activity and to determine the type of lymphocytes that appeared in the human endometrium. The primary human antibodies used in these analyses are summarized in Table I. A HISTFINE kit (Nichirei, Tokyo, Japan) and an EnVision kit (DakoCytomation, Inc., Carpinteria, CA, USA) were used to identify the human lymphocytes. Sections (1.5 μm) were deparaffinized and treated with methanol/3% hydrogen peroxide to block endogenous peroxidase. In order to retrieve masked antigens, the slides were immersed in citrate buffer (pH 6.0) and heated in an autoclave for 5 min at 121 °C. They were then incubated with primary antibody overnight, followed by biotinylated secondary antibody for 30 min and peroxidase-labelled streptavidin for 30 min. The antigen–antibody complex was visualized with 3,3′-diaminobenzidine (DAB) solution and counterstained with haematoxylin. Positive controls were samples of endometrial cancer (Ki-67), small-cell carcinoma (CD56), thymus (CD16) and normal human lymph nodes (CD3 and CD79α). The pairs of mirror-image sections were obtained simultaneously and stained for CD56 and CD16.

Double immunohistochemical labelling. The sections of day 28 were also labelled using a sequential double immunohistochemical staining for CD56 and CD3. Sections were incubated with CD56 overnight at first and the reaction was developed with DAB. After that, sections were incubated with CD3 overnight, and the reaction was developed with 4-chloro-1-naphthol.

Results

Transplantation

All of the NOG mice that received transplants of normal human endometrial tissue into the subcutaneous space survived and were sacrificed between 14 and 35 days after surgery. The success rate of xenotransplantation was 100% and the recovery rate of fragments was 94%. The two fragments transplanted into each mouse showed similar histological changes, which were not dependent upon the patient.

Histological assessment

Before transplantation, the endometrial tissue contained numerous small narrow glands with columnar glandular cells. Evidence of pseudostratification of the nuclei was also observed. The stroma was dense, and mitotic figures were identified in both the glandular and stromal cells. These findings indicate that the endometrial tissue was in the early proliferative phase (Figure 1A).

After 14 days, the tissues contained numerous small narrow glands with columnar glandular cells and pseudostratification of the nuclei. The stroma was dense, and many mitotic figures were observed in both the glandular and stromal cells (Figure 1B). These findings suggest that the cells were actively proliferating. The mean serum concentration of E_2 was 293.1 pg/ml at this stage.

By contrast, progressive development of secretory-phase characteristics was observed after treatment commenced with progesterone plus E_2. Subnuclear vacuolation of the glandular epithelium, the first detectable feature of the secretory phase, began to appear after 2 days of E_2 plus progesterone treatment (Figure 1C). The mean serum concentrations of E_2 and progesterone were 115 pg/ml and 12.0 ng/ml, respectively. By 21 days after transplantation, the glands were noticeably dilated and filled with fluid. In addition, the glandular cells appeared cuboidal and the pseudostratification of the nuclei had disappeared. Many lymphocytes were present throughout the stroma and tended to aggregate around the glands (Figure 1D). The mean serum concentrations of E_2 and progesterone were 158 pg/ml and 19.2 ng/ml, respectively. Progressive decidual change occurred in the stroma and marked decidualization was observed 28 days after transplantation. The typical late-secretory structure was present by this stage and numerous lymphocytes were identified throughout the stroma (Figure 1E). The mean serum concentrations of E_2 and progesterone were 54.5 pg/ml and 16.5 ng/ml, respectively.

Table I. Summary of the primary antibodies used in this study

Antibody (clone number)	Source	Optimal dilution	Antigen retrieval
Ki-67 (monoclonal: MIB-1)	Dako (Glostrup, Denmark)	1:50	Autoclave[a]
CD56 (monoclonal: 123C3)	Monosan (Am uden, The Netherlands)	1:80	Autoclave[a]
CD16 (monoclonal: 2H7)	Novo Castra (Newcastle, UK)	1:160	Autoclave[a]
CD3 (polyclonal)	Dako (Glostrup, Denmark)	1:500	Autoclave[a]
CD79α (monoclonal: JCB117)	Dako (Glostrup, Denmark)	1:40	Autoclave[a]

[a]Autoclave: heat in an autoclave for 5 min in citric acid buffer.

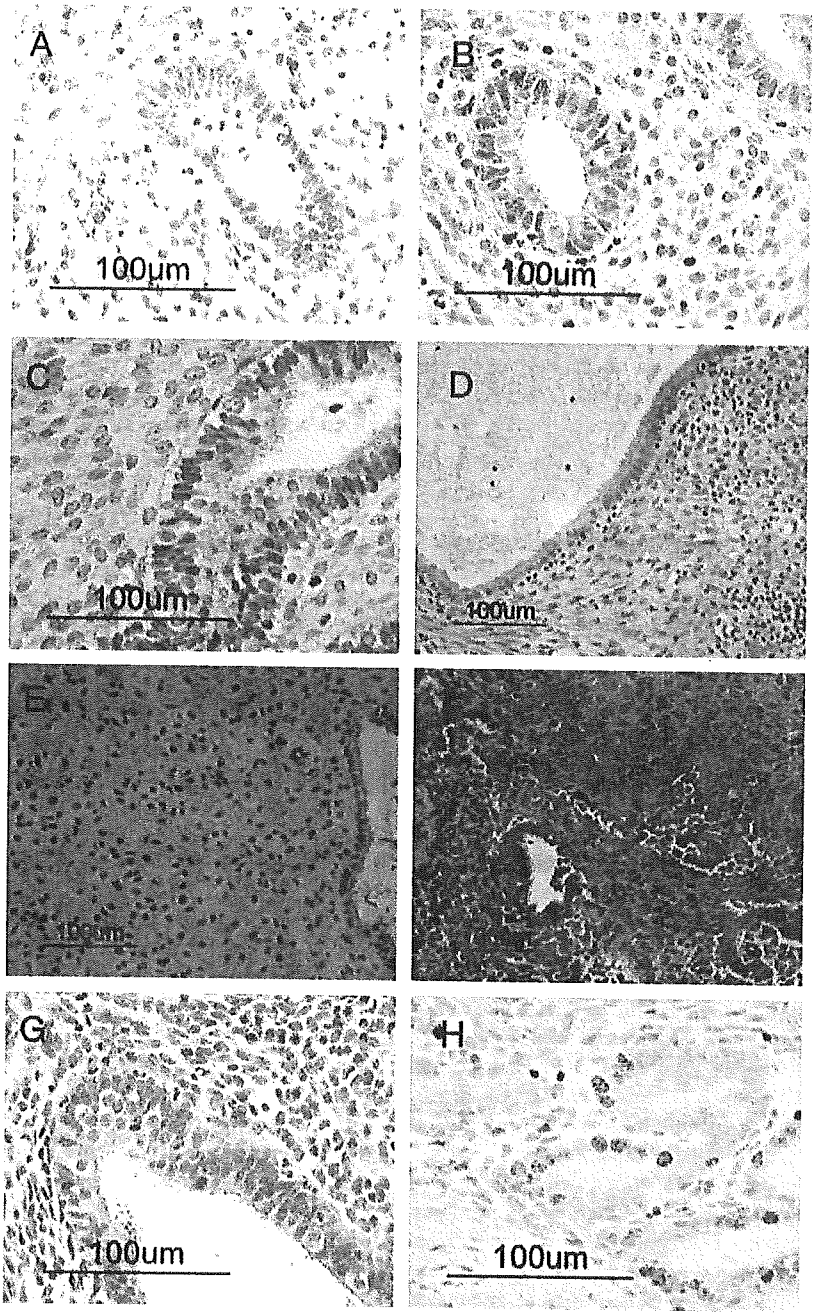

Figure 1. Histological sections stained with haematoxylin and eosin (**A**–**G**) and the immunohistochemical stain Ki-67 (**H**). (**A**) Pretransplantation endometrial tissue: the proliferative phase. The glands are small straight and narrow, with columnar glandular cells and prominent pseudostratification of the nuclei. The stromal cells are dense (magnification ×400). (**B**) Endometrial tissue 14 days after transplantation: E_2 has been administered for 14 days. The glands are small and narrow, with tall columnar cells. Evidence of pseudostratification of the nuclei is present. The stromal cells are dense (magnification ×400). (**C**) Endometrial tissue 16 days after transplantation: E_2 has been administered for 14 days, followed by E_2 plus progesterone for 2 days. The glands still show pseudostratified structures but they have begun to enlarge, and subnuclear vacuolation of the glandular cells is visible. The stromal cells remain dense (magnification ×400). (**D**) Endometrial tissue 21 days after transplantation: E_2 has been administered for 14 days, followed by E_2 plus progesterone for 7 days. The glands are significantly dilated, the glandular cells are cuboidal and the pseudostratification of the nuclei has disappeared. Stromal decidualization is beginning. Many lymphocytes are present throughout the stroma and are aggregating around the glands (magnification ×200). (**E**) Endometrial tissue 28 days after transplantation: E_2 has been administered for 14 days, followed by E_2 plus progesterone for 14 days. The glandular cells are cuboidal. Evidence of stromal decidualization is clearly seen and lymphocytes are present in the stroma (magnification ×200). (**F**) Endometrial tissue 31 days after transplantation: E_2 had been administered for 14 days, followed by E_2 plus progesterone for 14 days, and then no hormones for the remaining 3 days. The glands and endometrial stroma have collapsed during the evolution of the transplant. There is prominent bleeding in the stroma (magnification ×200). (**G**) Endometrial tissue 35 days after transplantation: E_2 had been administered for 14 days, followed by E_2